

AD-A190 010

NAVAL POSTGRADUATE SCHOOL Monterey, California



THESIS

DTIC
ELECTE
MAR 11 1988
S D

EFFECT OF FRICTION AND CONTROL
PARAMETERS
ON THE TRACKING ACCURACY OF A TARGET
SEEKER

by
Joseph K. Chan

December 1987

Thesis Advisor Anthony J. Healey

Approved for public release; distribution is unlimited.

88 3 10 024

A190010

REPORT DOCUMENTATION PAGE

1a REPORT SECURITY CLASSIFICATION Unclassified			1b RESTRICTIVE MARKINGS		
2a SECURITY CLASSIFICATION AUTHORITY			3 DISTRIBUTION/AVAILABILITY OF REPORT		
2b DECLASSIFICATION/DOWNGRADING SCHEDULE			Distribution unlimited		
4 PERFORMING ORGANIZATION REPORT NUMBER(S)			5 MONITORING ORGANIZATION REPORT NUMBER(S)		
6a NAME OF PERFORMING ORGANIZATION Naval Postgraduate School		6b OFFICE SYMBOL (if applicable)	7a NAME OF MONITORING ORGANIZATION Naval Postgraduate School		
6c ADDRESS (City, State, and ZIP Code) Monterey, California 93943-5100			7b ADDRESS (City, State, and ZIP Code) Monterey, California 93943-5100		
8a NAME OF FUNDING SPONSORING ORGANIZATION		8b OFFICE SYMBOL (if applicable)	9 PROCUREMENT INSTRUMENT IDENTIFICATION NUMBER		
8c ADDRESS (City, State, and ZIP Code)			10 SOURCE OF FUNDING NUMBERS		
		PROGRAM ELEMENT NO	PROJECT NO	TASK NO	WORK UNIT ACCESSION NO
11 TITLE (Include Security Classification) EFFECT OF FRICTION AND CONTROL PARAMETERS ON THE TRACKING ACCURACY OF A TARGET SEEKER (U)					
12 PERSONAL AUTHOR(S) Chan, Joseph K.					
13a TYPE OF REPORT Master's Thesis		13b TIME COVERED FROM TO		14 DATE OF REPORT (Year, Month, Day) 1987 December 15	15 PAGE COUNT 75
16 SUPPLEMENTARY NOTATION					
17 COSM CODES			18 SUBJECT TERMS (Continue on reverse if necessary and identify by block number)		
FIELD	GROUP	SUB-GROUP	Friction, Model-reference, P.D. control, P.I.D. control, Tracking accuracy, Target seeker		
19 ABSTRACT (Continue on reverse if necessary and identify by block number)					
<p>The tracking accuracy of a missile target seeker depends on many variables. For a target seeker using a gimballed platform, an important variable is the friction induced by the preloaded bearings, and by the short wires which connect the target detector with the rest of the seeker's electronics. This friction force is nonlinear and sufficiently large enough such that accurate position tracking of a target, whether stationary or moving, is difficult. Conventional control methods such as P.D. (proportional plus derivative) or P.I.D. (proportional plus derivative plus integral) control action can not satisfactorily meet the error criteria. To overcome the deficiency of these two methods, a model-reference method has been synthesized, relying on idealized predictor corrector control to improve the tracking accuracy of the missile seeker. Computer simulations using the Dynamic Simulation Language have demonstrated the superior performance expected from this method.</p>					
20 DISTRIBUTION/AVAILABILITY OF ABSTRACT <input checked="" type="checkbox"/> UNCLASSIFIED UNLIMITED <input type="checkbox"/> SAME AS RPT <input type="checkbox"/> DTIC USERS			21 ABSTRACT SECURITY CLASSIFICATION Unclassified		
22a NAME OF RESPONSIBLE INDIVIDUAL A. J. Healey			22b TELEPHONE (Include Area Code) 2032	22c OFFICE SYMBOL 39	

Approved for public release; distribution is unlimited.

**EFFECT OF FRICTION AND CONTROL PARAMETERS
ON THE TRACKING ACCURACY OF A TARGET SEEKER**

by

Joseph K. Chan
Naval Weapons Center, China Lake, California
B.S., University of South Alabama, 1981

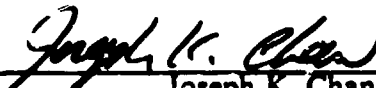
Submitted in partial fulfillment of the
requirements for the degree of

MASTER OF SCIENCE IN MECHANICAL ENGINEERING

from the

**NAVAL POSTGRADUATE SCHOOL
December 1987**

Author:



Joseph K. Chan

Approved by:



Anthony J. Healey, Thesis Advisor



Anthony J. Healey, Chairman,
Department of Mechanical Engineering



Gordon Schacher,
Dean of Science and Engineering

ABSTRACT

The tracking accuracy of a missile target seeker depends on many variables. For a target seeker using a gimbaled platform, an important variable is the friction induced by the preloaded bearings, and by the short wires which connect the target detector with the rest of the seeker's electronics. This friction force is nonlinear and sufficiently large enough such that accurate position tracking of a target, whether stationary or moving, is difficult. Conventional control methods such as P.D. (proportional plus derivative) or P.I.D. (proportional plus derivative plus integral) control action can not satisfactorily meet the error criteria. To overcome the deficiency of these two methods, a model-reference method has been synthesized, relying on idealized predictor corrector control to improve the tracking accuracy of the missile seeker. Computer simulations using the Dynamic Simulation Language have demonstrated the superior performance expected from this method.



Accession For	
NTIS CRA&I	<input checked="" type="checkbox"/>
DTIC TAB	<input type="checkbox"/>
Unannounced	<input type="checkbox"/>
Justification	
By	
Distribution/	
Availability Codes	
Dist	Avail and/or Special
A-1	

TABLE OF CONTENTS

I.	INTRODUCTION	8
A.	BACKGROUND	8
B.	RECENT DEVELOPMENTS IN CONTROL	9
C.	OBJECTIVE	10
D.	METHOD AND APPROACH	10
II.	ANALYTICAL MODELING	11
A.	INTRODUCTION	11
B.	EQUATION OF MOTION	11
C.	FRICTION MODEL	12
D.	BLOCK DIAGRAM OF BASIC CONTROL SYSTEM	14
E.	MODEL-REFERENCE CONTROL	16
F.	INPUT SIGNAL MODEL	17
III.	COMPUTER SIMULATION METHOD	20
A.	INTRODUCTION	20
B.	GEOMETRIC DESCRIPTION	20
C.	ACCELERATION SIMULATION	20
D.	DSL CODING	20
IV.	SIMULATION RESULTS	23
A.	INTRODUCTION	23
B.	EFFECT OF FRICTION ON ACCURACY	23
C.	EFFECT OF THE K_1	33
D.	EFFECT OF SPRING CONSTANT	33
E.	EFFECT OF INTEGRAL GAIN TIME CONSTANT	42
F.	EFFECT OF G_1	42
G.	EFFECT OF μ PREDICTION ERROR	51
H.	EFFECT OF UNBALANCED SYSTEM	51
I.	EFFECT OF ACCELERATION	60

V.	DISCUSSION AND RECOMMENDATION	65
A.	INTRODUCTION	65
B.	DISCUSSION	65
C.	RECOMMENDATION	66
APPENDIX A:	DSL LISTINGS (PD, PID CONTROL)	67
APPENDIX B:	DSL LISTINGS (PC CONTROL)	70
	LIST OF REFERENCES	73
	INITIAL DISTRIBUTION LIST	74

LIST OF FIGURES

1.1	Typical Seeker Configuration	9
2.1	Free Body Diagram of the Platform	12
2.2	Friction Model of the Bearings and Wires	13
2.3	Response of the Friction Model	14
2.4	Block Diagram	15
2.5	Model-Reference Control Action	18
3.1	D.S.L. Program Flowchart	22
4.1	Balanced System, PD Control, No Friction	25
4.2	$\mu = 0.1, K_1 = 15.0, K_2 = 0.5, \delta = 0.05$	26
4.3	$\mu = 0.2, K_1 = 15.0, K_2 = 0.5, \delta = 0.05$	27
4.4	$\mu = 0.3, K_1 = 15.0, K_2 = 0.5, \delta = 0.05$	28
4.5	$\mu = 0.1, K_1 = 15.0, K_2 = 0.5, \delta = 0.05$, PID Control $T_i = 1.0$	29
4.6	$\mu = 0.2, K_1 = 15.0, K_2 = 0.5, \delta = 0.05$, PID Control $T_i = 1.0$	30
4.7	$\mu = 0.3, K_1 = 15.0, K_2 = 0.5, \delta = 0.05$, PID Control $T_i = 1.0$	31
4.8	Position Error Vs Gain Constant K_1	32
4.9	$\mu = 0.3, K_1 = 2.0, \delta = 0.05$	34
4.10	$\mu = 0.3, K_1 = 5.0, \delta = 0.05$	35
4.11	$\mu = 0.3, K_1 = 15.0, \delta = 0.05$	36
4.12	$\mu = 0.3, K_1 = 15.0, \delta = 0.05$, Sin Input	37
4.13	$\mu = 0.3, K_1 = 30.0, \delta = 0.05$, Sin Input	38
4.14	$\mu = 0.3, K_1 = 1000.0, \delta = 0.05$, Sin Input	39
4.15	$\mu = 0.3, K_1 = 5.0, \delta = 0.001$	40
4.16	$\mu = 0.3, K_1 = 5.0, \delta = 0.01$	41
4.17	$\mu = 0.3, K_1 = 5.0, \delta = 0.1$	43
4.18	Balanced System, PD Control, No Friction, Sin Input	44
4.19	$\mu = 0.3, K_1 = 5.0, \delta = 0.01$, Sin Input	45
4.20	$\mu = 0.3, K_1 = 5.0, \delta = 0.1$, Sin Input	46
4.21	$\mu = 0.1, K_1 = 15.0, \delta = 0.05$, PID Control, $T_i = 2$	47

4.22	$\mu = 0.1, K_1 = 15.0, \delta = 0.05, \text{PID Control, } T_i = 3$	48
4.23	$\mu = 0.3, K_1 = 30.0, \delta = 0.05, \mu_m = 0.3, \delta_m = 0.05, G_1 = 30.0$	49
4.24	$\mu = 0.3, K_1 = 30.0, \delta = 0.05, \mu_m = 0.3, \delta_m = 0.05, G_1 = 500.0$	50
4.25	$\mu = 0.3, K_1 = 15.0, \delta = 0.05, \mu_m = 0.3, \delta_m = 0.05, G_1 = 3000.0$	52
4.26	$\mu = 0.1, K_1 = 15.0, \delta = 0.05, \mu_m = 0.3, \delta_m = 0.05, G_1 = 3000.0$	53
4.27	$\mu = 0.2, K_1 = 15.0, \delta = 0.05, \mu_m = 0.3, \delta_m = 0.05, G_1 = 3000.0$	54
4.28	$\mu = 0.4, K_1 = 15.0, \delta = 0.05, \mu_m = 0.3, \delta_m = 0.05, G_1 = 3000.0$	55
4.29	$\mu = 0.5, K_1 = 15.0, \delta = 0.05, \mu_m = 0.3, \delta_m = 0.05, G_1 = 3000.0$	56
4.30	$\mu = 0.3, K_1 = 15.0, \delta = 0.05, \text{PD Control, } Z_m = 3864.0, Y_o = 0.1,$ $Z_o = 0.2$	57
4.31	$\mu = 0.3, K_1 = 15.0, \delta = 0.05, \text{PD Control, } Z_m = 3864.0, y_o = 0.2,$ $Z_o = 0.4$	58
4.32	$\mu = 0.3, K_1 = 15.0, \delta = 0.05, \text{PD Control, } Z_m = 3864.0, y_o = 0.2,$ $Z_o = 0.6$	59
4.33	$\mu = 0.3, K_1 = 15.0, \delta = 0.05, Z_m = 3864.0, \text{PD Control, step response}$	61
4.34	$\mu = 0.3, K_1 = 15.0, \delta = 0.05, Z_m = 3864.0, \text{PD Control, sin response}$	62
4.35	$\mu = 0.3, K_1 = 15.0, \delta = 0.05, Z_m = 3864.0, \text{M-F Control, step response}$	63
4.36	$\mu = 0.3, K_1 = 15.0, \delta = 0.05, Z_m = 3864.0, \text{M-F Control, sin response}$	64

I. INTRODUCTION

A. BACKGROUND

A typical air-to-air missile seeker might consist of a set of focusing optics, a detector, signal processing electronics, gyros, rate and position sensors, all mounted on a gimbaled platform as illustrated in Figure 1.1. A missile target seeker's function is to detect and to track a target, whether stationary or moving, until the target is neutralized. There are many variables which affect the accuracy of the seeker. Mechanical variables include friction, inertia, location of center of gravity, and vibration. Electrical variables include servos, signal processing limitations, and noise. Other variables such as thermal noise, external disturbances, electro-magnetic interferences, all play an important role in the tracking accuracy of a missile seeker. One of the most important considerations is the effect of friction on the tracking accuracy. For a seeker with a gimbaled platform, the friction primarily comes from the preloaded bearings and from the wires connecting the platform electronics and the seeker electronics located off the platform. This type of friction is nonlinear and its direction changes in relation to the motion of the target. Excessive friction causes "sticking" behavior and impairs accurate tracking.

Control of the position of a massive object in the presence of friction is not an easy task and requires high positional feedback gain with accompanying high drive stiffness for accuracy. Not only does this problem arise in target seekers, but also in optical tracking telescopes, and robotic manipulators. Classical control techniques for accurate tracking have been based on the provision of a drive torque being proportional to angular position error with dynamic compensation based on integral and/or derivative action. Target position is sensed by the optical apparatus as an angular error from the straight line pointing vector. Platform drive torques are then commanded to drive the angular pointing error to zero so that the angular position of the gimbaled platform automatically aligns with the target. In stabilizing dynamic motions, rate feedback from platform is essentially provided by either the gyros or by a resolver mounted opposite the torque motor on the platform. The accuracy of tracking is limited by the sensitivity of the feedback elements and is further impaired by vibration and sensor noise [Ref. 1] Normally, high positional feedback gain results in a

high drive stiffness, but, with the presence of vibration and noise, high stiffness increases errors. Modern stabilization techniques are being sought that overcome the need for high feedback gains.

In this thesis, the use of a model based predictor corrector control has been demonstrated, including the use of a "stick-slip" friction model for predicting the added torque required to compensate for frictional induced inaccuracies.

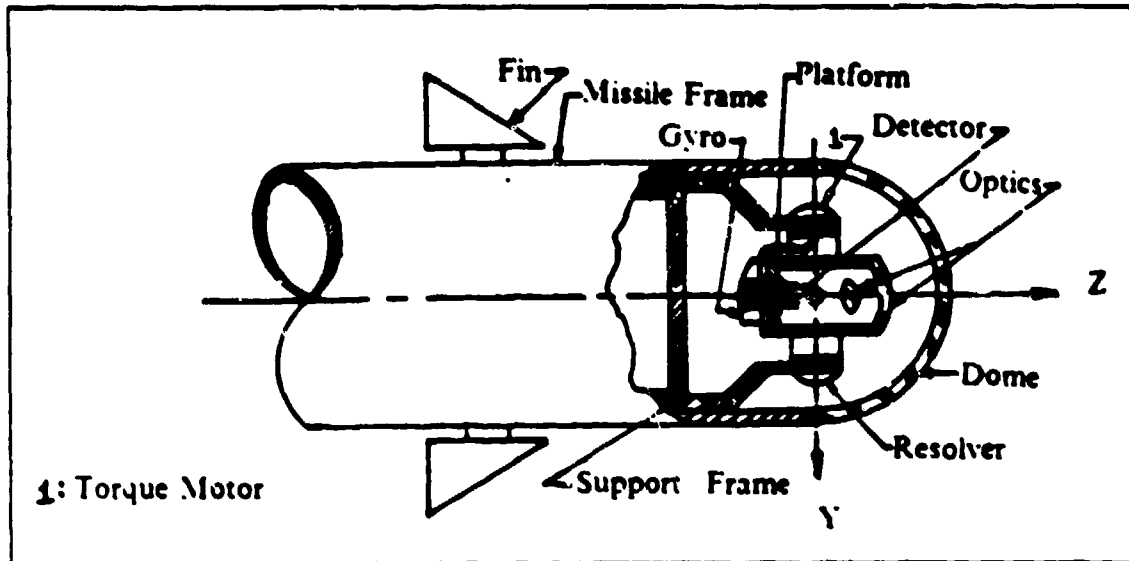


Figure 1.1 Typical Seeker Configuration.

B. RECENT DEVELOPMENTS IN CONTROL

A typical method employed to control the position error of a mechanical system is the P.D. (proportional plus derivative) action. This control scheme works well in most control applications but it has one drawback, the presence of steady state error. Integral action is usually added to eliminate the steady state error, but it is useless in the presence of non-linearity elements. Lag lead compensation technique is usually employed to overcome non-linearity effects by increasing the gain in the system and subsequently lead to increase noise in the system and increase error.

The use of model-reference controls increased in recent years. It is found that this technique lends itself to the problem of controlling complex and often non-linear systems. With the advent of modern microprocessor based controls, techniques using model following controls [Ref. 2] offer advantages where a large part of the control

force and effect can be predicted, rather than relying on feedback methods alone for correction of errors. Model Reference Controls have been used as an ideal response generator for comparison with actual system response so that plant parameter changes can be monitored, identified, and control gains adjusted automatically. Additionally, with particular emphasis on nonlinear systems in robotics, the computed torque method and sliding mode control design [Ref. 3] have been proposed for providing improved model following and tracking system performance.

C. OBJECTIVE

The effectiveness of a target tracker depends on its ability to maintain the target within its line of sight regardless of the actions taken by the target. This requires a high degree of accuracy on the part of the seeker to respond to the motion of the target. It is demonstrated that friction, among other impediments, reduces the ability of the seeker to track a target. It is the purpose of this investigation to compare tracking performance with both classical P.I.D., P.D., and model-reference control actions under the assumption of deterministic signals. The primary disturbance is considered to arise from friction which is modeled here to include coulomb friction and the elastic effects from wiring harnesses.

D. METHOD AND APPROACH

The approach to this problem begins with a study of the friction variables and their effect on the tracking error. Then, the performance of the classical control actions, P.D., P.I.D. is evaluated. Finally, a model-reference method has been synthesized to improve the tracking accuracy of the seeker. All evaluations were done by computer simulation using the Dynamic Simulation Language (D.S.L.) developed for the I.B.M. 3033 computer. The simulation is limited to a single degree of freedom gimbal and it is shown that superior tracking accuracy may be achieved using a model-reference system with nonlinear friction force compensation.

II. ANALYTICAL MODELING

A. INTRODUCTION

This chapter discusses the development of the mathematical model for the target seeker dynamics in one degree of freedom and the reference model used for nonlinear friction compensation. The analytical modeling begins with the derivation of the equations of motion for the platform in the Y-Z plane. The motions in the other planes are neglected at this time to reduce the level of complexity. Even with this simplification, the information obtained in this study should prove useful in gaining an insight to the interaction of friction in a dynamic system. A friction model based on a "stick-slip" concept will be developed to model the combined friction effect of the bearings and wire harness. This is followed by the presentation of the classical control actions. A model-reference method to control the position error will be synthesized to improve the tracking accuracy. A brief discussion of the input signal model will complete this chapter.

B. EQUATION OF MOTION

The platform, together with the optics, detector, gyros, signal processing electronics and sensors can be modeled as a simple cylinder with a small degree of out of balance. The analysis begins with the determination of the forces acting on the system as shown in Figure 2.1. Using Newton's second law of motion and D'Alembert's Principle, the equation of motion of the seeker is derived as,

$$(I_m + mr^2) \ddot{\theta} + F(\theta, \dot{\theta}) + m\ddot{z}r(\cos\theta\cos\phi - \sin\theta\sin\phi) = T_x \quad (\text{eqn 2.1})$$

where the torque, T_x , required to move the platform through an angular displacement, θ , depends on the position and velocity of the platform and on the motor's characteristics. The friction term in this equation is nonlinear. It is a function of θ and $\dot{\theta}$. The terms in \ddot{z} refer to an axial acceleration induced torque arising from some small out of balance mass m located at a distance r from the geometric center making an angle ϕ from the Y axis.

With a typical d.c. motor, the output torque can be expressed for purposes of position control as the sum of proportional error and rate terms, as,

$$T_x = K_1(\theta_c - \theta) - K_2\dot{\theta} \quad (\text{eqn 2.2})$$

where K_1 is the motor gain constant and K_2 is the velocity gain constant. For an input command, θ_c , the required torque can be calculated by Equation 2.2 if the displacement θ and velocity $\dot{\theta}$ of the platform are known. The damping ratio $\zeta < 2$ is used to provide proper damping of the system.

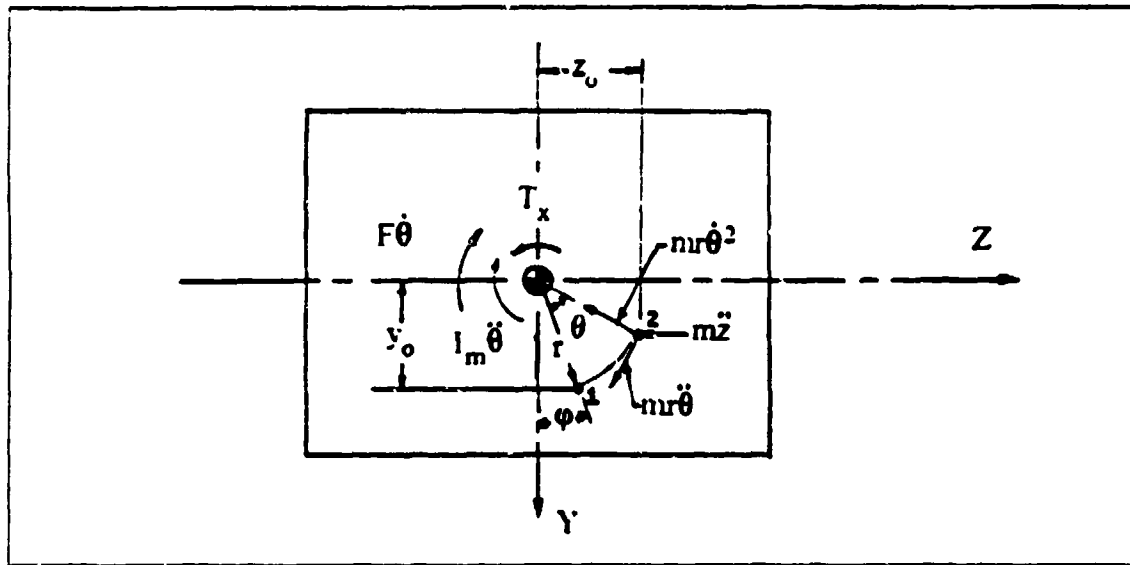


Figure 2.1 Free Body Diagram of the Platform.

C. FRICTION MODEL

The main contributors of friction in this platform are the bearings and the electrical wires which connect the platform electronics with that located in the support structure. A proper friction model must begin with the understanding of how these two components behave. The bearing friction is basically rolling friction which is a function of the surface roughness of the races and of the angular speed of the platform. The wires act as a spring which could be quite stiff when they are bundled, or soft when they are loose. Relative motion between wires in a harness causes an additional friction force that is dependent on the stiffness of the harness. The combined friction

from the two components can be modeled as a massless slider with a spring attached to it as shown in Figure 2.2.

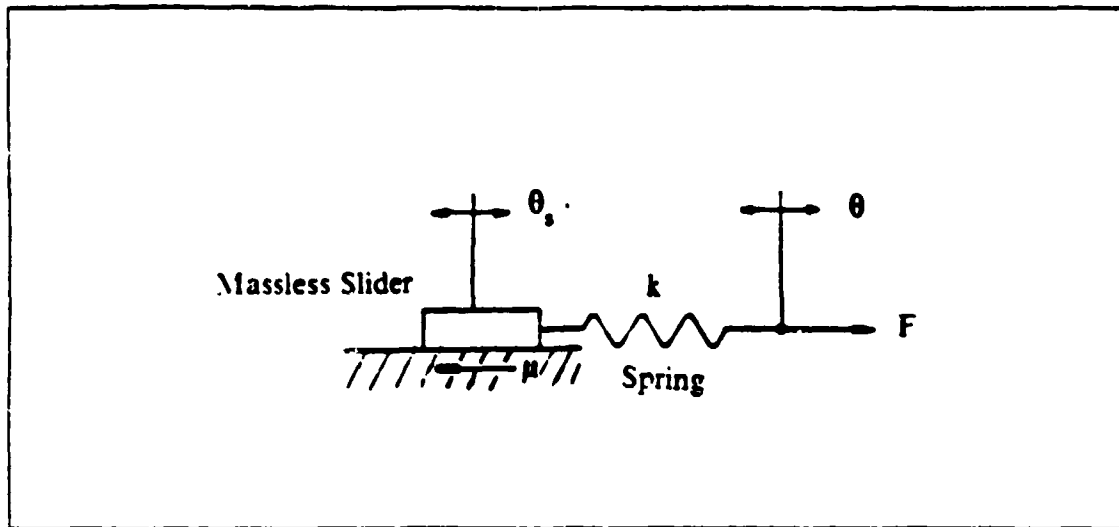


Figure 2.2 Friction Model of the Bearings and Wires.

The force pulling on the spring stretches the spring by a distance θ until the spring's potential force is overcome. Then, the slider begins to move to a distance θ_s . The friction force then is equal to the product of the spring constant and the net motion $(\theta - \theta_s)$ of the spring. The spring constant, k , is a function of the coefficient of friction between the slider and the surface, μ , and of the amount of the allowable stretch on the spring, δ . A large value for δ represents a soft spring; and a small value for δ represents a stiff spring. When the direction is reversed, the force pushes on the spring, compressing it until the force is greater than the spring's potential force and the slider moves in the opposite direction. The friction force of this model is given as,

$$F = \frac{\mu(\theta - \theta_s)}{\delta} \quad (\text{eqn 2.3})$$

When the friction force is less than the friction between the two surfaces, the slider does not move until the friction force increases to exceed μ as indicated in 2.4 and 2.5.

$$\theta_s = \theta_s \quad F < \mu \quad (\text{eqn 2.4})$$

$$\dot{\theta}_s = \dot{\theta}_s - \delta \frac{F}{\text{ABS}(F)} \quad F > \mu \quad (\text{eqn 2.5})$$

In reality, a friction force can exist even though there is no relative motion. A closer look at equation 2.3 reveals the ability of this model to support a non-zero friction force. When $\dot{\theta}_s$ is zero, that is, the platform is not rotating, the friction force is equal to the product of the spring constant and θ . A typical coulomb friction model would have a zero friction force when $\dot{\theta}_s$ is zero. It is the ability of this model to handle nonzero friction force which sets it apart from conventional coulomb friction model. Once the force exceeds the friction force, the slider starts to move with its direction determined by the direction of the force as indicated in Equations 2.5. The response of the slider-spring friction model is illustrated in Figure 2.3.

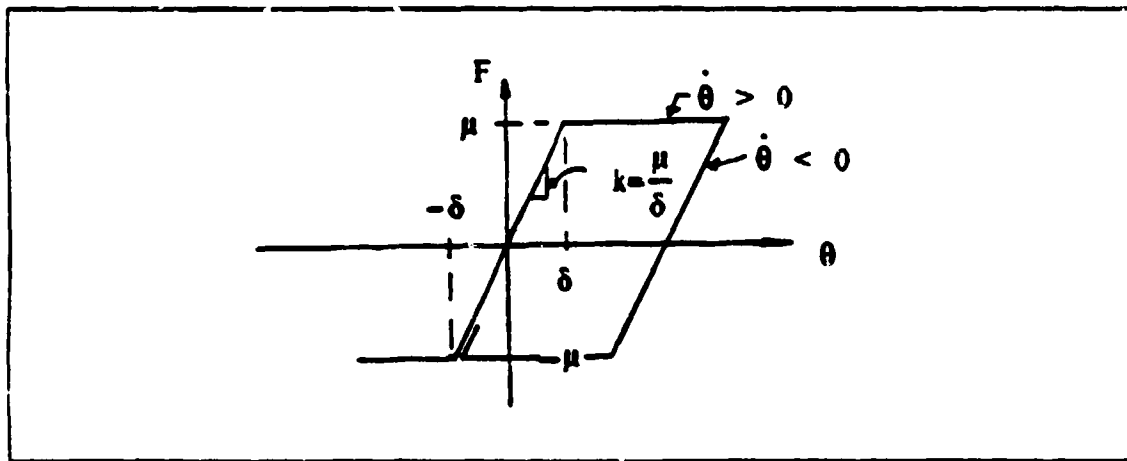


Figure 2.3 Response of the Friction Model.

D. BLOCK DIAGRAM OF BASIC CONTROL SYSTEM

The behavior of the system can now be put in a more convenient form for control analysis and simulation. A block diagram is constructed from Equations 2.1 and 2.2. Figure 2.4 provides an visual interpretation of the control system which allows more effective analysis of the problem.

The command signal, θ_c , is compared with the position feedback signal, θ , to produce an error ϵ . This signal is amplified by a feedforward gain K_1 in the P.D. control method. The amplified signal is compared with the velocity feedback signal to produce

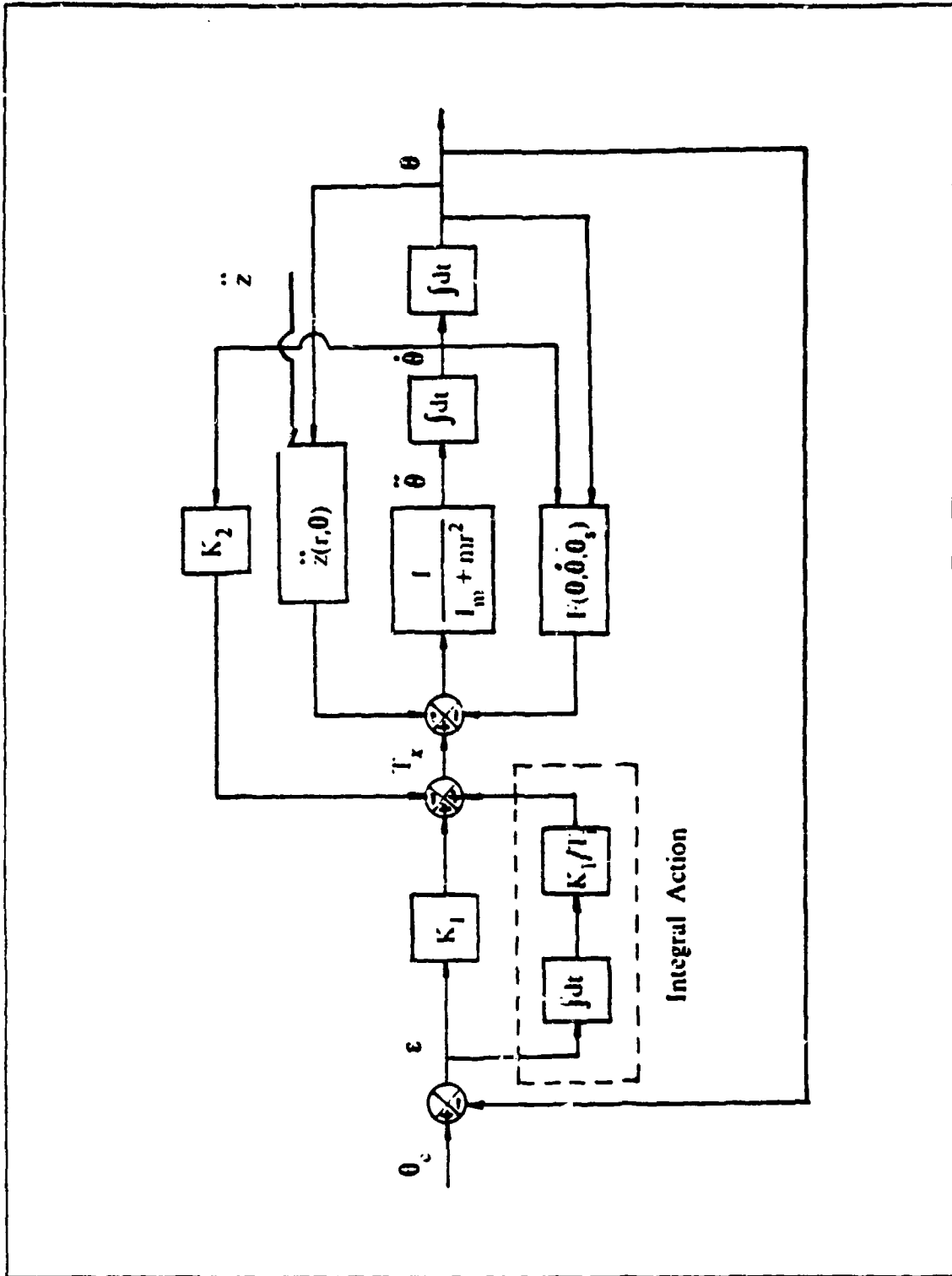


Figure 2.4 Block Diagram

the required torque to drive the platform. However, this torque is reduced by the friction torque caused by the bearings and wires. The torque generated by the out of balance mass reduces the available torque even further. What is left is a greatly reduced torque which is not necessarily high enough to drive the platform dynamics to the desired position and a position error exists. P.D. control action simply would not produce a zero position error. The shortcoming of this scheme is its lack of history of how the error changes with time. The integral action, shown as dotted outlines in Figure 2.4, helps to reduce the error by summing errors accumulated up to the most recent time, then an amplified average of this error is added to produce the required torque. The overall effect is better error reporting and correcting. Ideally, this method would produce zero position error. Both the P.D. and P.I.D. control suffer noise sensitivity problems. When a noise, either internal or external, is introduced to the system it is amplified by the control actions and accurate tracking becomes difficult.

E. MODEL-REFERENCE CONTROL

Consider an ideal system which has the same basic inertial characteristics as the platform. This is referred to as a model. Assuming the model is perfectly balanced and neglecting the effect of friction, the ideal model dynamics is expressed by Equation 2.6.

$$X = \frac{U}{I_m + mr^2} \quad (\text{eqn 2.6})$$

If this model is rotated by a motor with the output torque expressed as the sum of a positional error and rate feedback, the torque equation is given as,

$$U = G_1(\theta_c - X) - G_2\dot{X} \quad (\text{eqn 2.7})$$

where U is the ideal motor output torque, θ_c is the command signal as defined before. X and \dot{X} denotes the position and velocity of the model, respectively. G_1 is the positional error gain and G_2 is the velocity feedback gain. The value of G_1 is limited only by the deliverable torque from the torque motor and G_2 follows the same damping rule as K_2 but without the problem of signal noise generation. The model friction due to the bearings and wires can be modeled as before. Using the notation X in place of θ , \dot{X} in place of $\dot{\theta}$, μ_m and δ_m replace μ and δ . the model friction is expressed by Equation 2.8.

$$F_m = \frac{\mu_m(X - X_s)}{\delta_m} \quad (\text{eqn 2.8})$$

$$X_s = X_s \quad F_m < \mu_m \quad (\text{eqn 2.9})$$

$$X_s = X_s - \delta_m \frac{F_m}{\text{ABS}(F_m)} \quad F_m > \mu_m \quad (\text{eqn 2.10})$$

In order to overcome the friction torque and drive the model to θ_c , the torque needed must be the sum of the two torques described above. The predicted torque is given below,

$$T_{xpred} = U + F_m \quad (\text{eqn 2.11})$$

To correct for any positional and velocity errors that might exist between the model and the platform, an additional correction torque based on the amplified error signals are added to the predicted torque to yield the total required torque, expressed in Equation 2.12 as,

$$T_x = T_{xpred} + K_1(X - \theta) + K_2(\dot{X} - \dot{\theta}) \quad (\text{eqn 2.12})$$

where the second term corrects the positional error and the third term corrects the velocity error.

This software based model is described in Figure 2.5. It is assumed that the torque to drive the platform in following command signals can be expressed as the sum of the torque to drive an ideal platform with no friction plus the torque required to overcome friction as established by the ideal platform model. Since the actual platform motion may differ slightly from that of the ideal, a correction torque is added based on a proportional and derivative action applied to motion errors.

F. INPUT SIGNAL MODEL

The response of the system to a step input and a sine input is simulated using the D.S.L. simulation program. An input command is 0.2 radians for all simulations. This is equivalent to commanding the seeker to move 11.459 degrees. The step input is roughly equal to an initial target acquisition phase which the seeker is required to lock

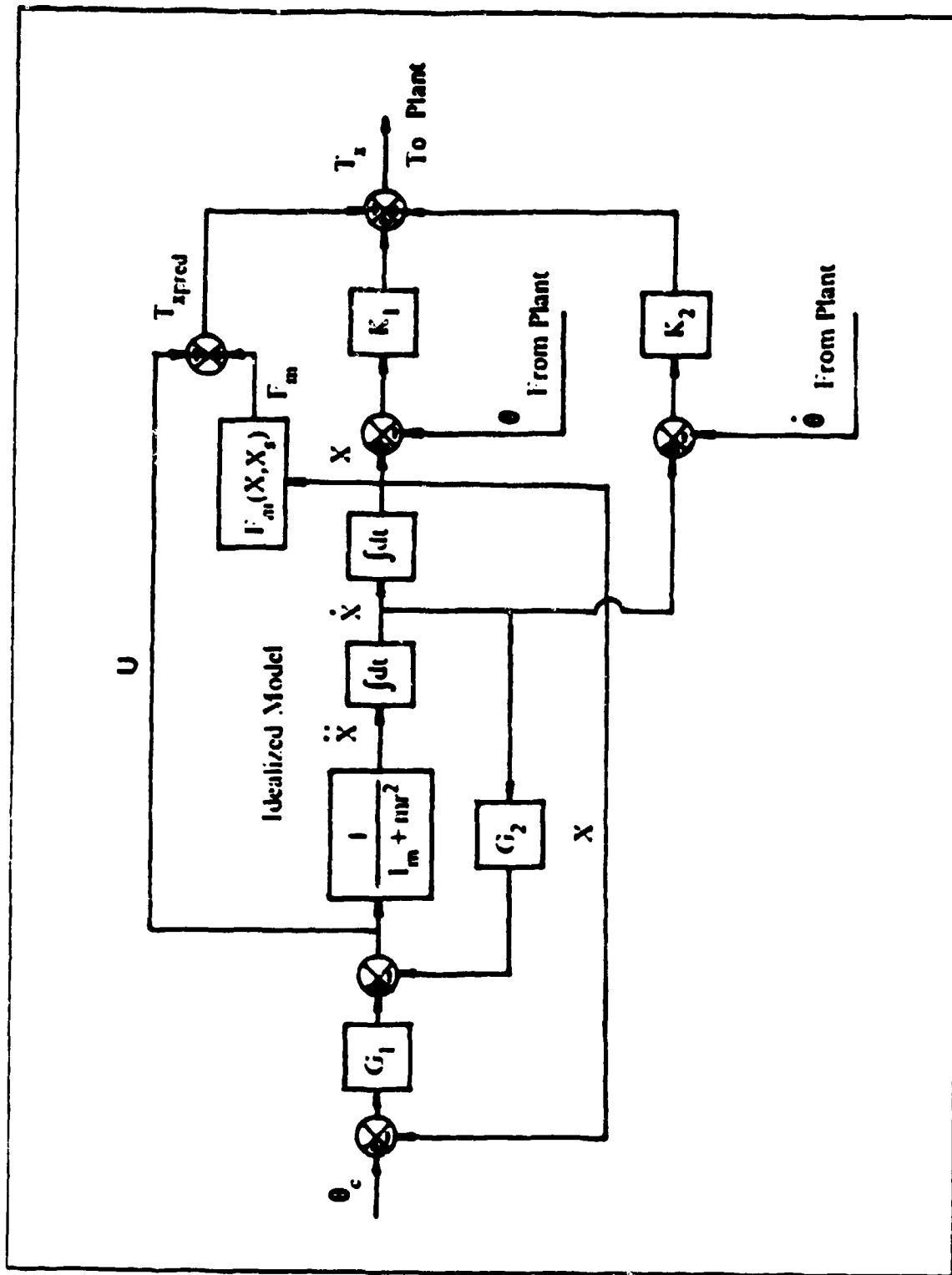


Figure 2.5 Model-Reference Control Action

on to the target or when the target is stationary. The sinusoidal input simulates the maneuvering of the target to avoid lock on. The target is assumed to be moving at 2.5 Hz. This type of maneuver is extreme because most targets are not able to evade this quickly. However, most missiles flex and rotate while moving through the air, which makes this assumption more realistic.

III. COMPUTER SIMULATION METHOD

A. INTRODUCTION

Dynamic Simulation Language (D.S.L.) is a FORTRAN-based simulation language for simulation of continuous systems. Its strength lies in its built in functions which allow the composition and simulation of any physical systems. Some of the built in functions include integrators, function generators, non-linear functions, probability distribution functions, and linear transfer functions; allow easy construction and simulation of the system without heavy programming. A more comprehensive look at the capabilities of D.S.L. can be found in References 4 and 5.

B. GEOMETRIC DESCRIPTION

The platform was modeled as an cylinder two inches in diameter and three and a half inches in height. The total mass of the cylinder was 0.0029 slugs plus a 10% out of balance mass (0.0003 slugs). The inertia of the cylinder was 0.0037 lb-in-s². The initial distance of the out of balance mass from the geometric center was taken to be 0.1 inches in the positive Y direction and 0.2 inches in the positive Z direction. This distance as well as the friction and control parameters were varied to determine their effects on the performance of the seeker.

C. ACCELERATION SIMULATION

The effect of acceleration is simulated under an assumed flight profile. The maximum acceleration subjected to the platform is assumed to be an exponential function describes by Equation 3.1 and 3.2.

$$Z = Z_m(1-\text{EXP}\{-t/\tau_1\}) \quad t < \tau_1 \quad (\text{eqn 3.1})$$

$$Z = Z_m \text{EXP}\{-t/\tau_2\} \quad t > 4\tau_1 \quad (\text{eqn 3.2})$$

where τ_1 and τ_2 are some arbitrary constants.

D. DSL CODING

The flow chart shown in Figure 3.1 illustrates the basic structure of the D.S.L. program used in the simulation of the seeker. The program is divided into segments:

TITLE, CONSTANT, PARAMETER, INITIAL, DYNAMIC, DERIVATIVE, AND TERMINAL. The **TITLE** segment named the program. The **CONST** segment defines the constants in the program which include the mass properties of the seeker and the maximum acceleration. **PARAM** segment defines the constants which will be changed from one simulation run to the next. It defines the friction characteristics of the seeker model, input signals, time constants, gain constants, and the geometry of the out of balance mass. The **INITIAL** segment initializes the variables and calculates the values of the out of balance geometry and velocity feedback constant. The **DYNAMIC** segment calculates the acceleration profile of the seeker and the input signals. This segment is computed at each time steps. The **DERIVATIVE** segment is the main body of the program. It consists of the description of the seeker dynamics as well as the control actions being used. Finally, the last segment, **TERMINAL**, contains the commands with regard to the total simulation time desired as well as the printing and plotting information.

Appendix A presents the DSL programming codes for the simulation of the classical P.D. and P.I.D. control actions and Appendix B presents the DSL programming code for the model-reference control method. The symbol "*" means the line is not used for current simulation.

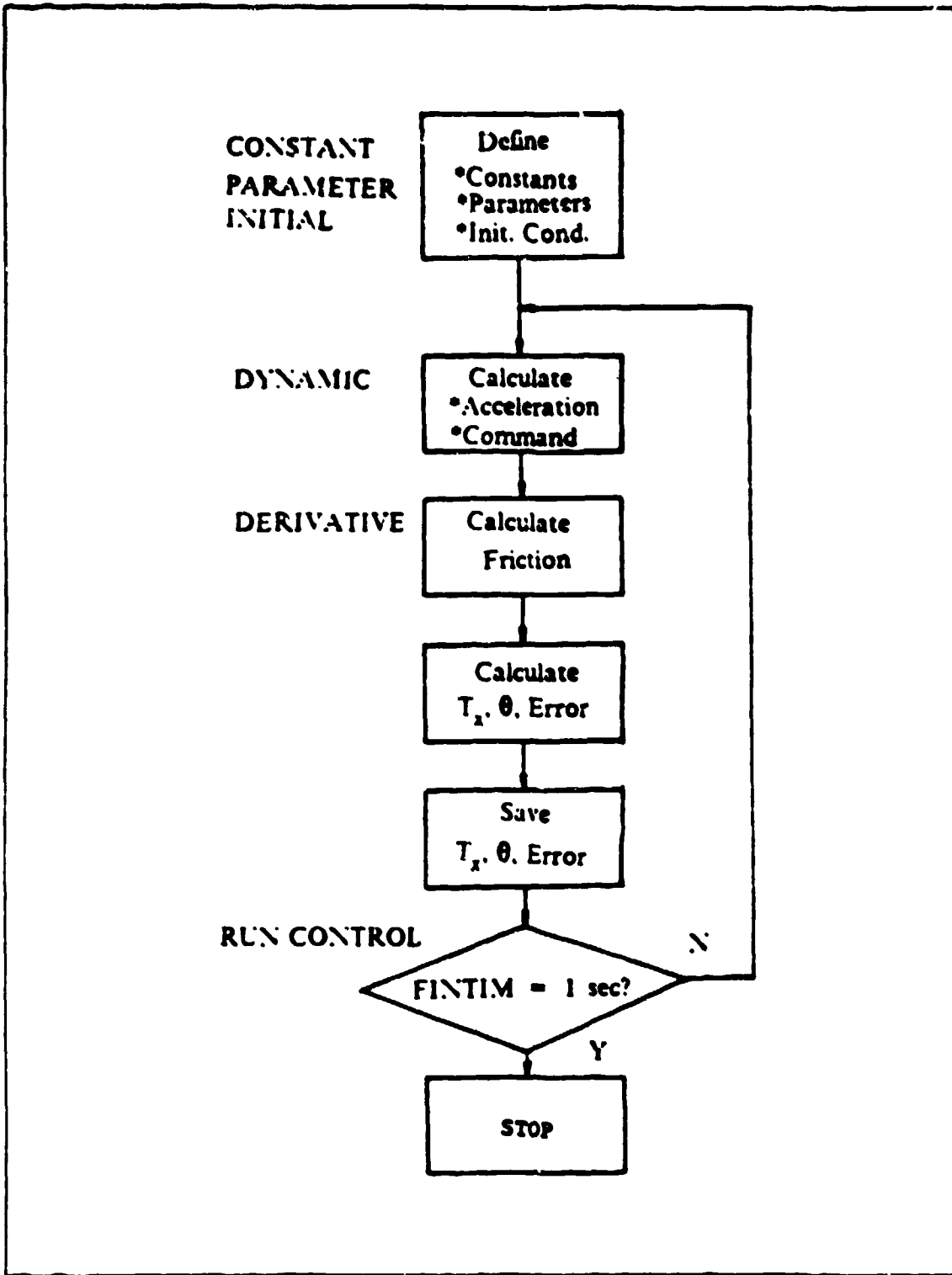


Figure 3.1 D.S.L. Program Flowchart

IV. SIMULATION RESULTS

A. INTRODUCTION

This chapter presents the results of the simulation. The effect of friction, control parameters, and control schemes on the tracking accuracy are illustrated by accompanying figures. Except as indicated, all figures shown the command signal, θ_c , as a series of short dashes and the actual response, θ (TH), as a solid line. The actual torque, T_x (TX) was indicated as medium length dash lines. Most of the figures reflect the response to the sinusoidal input, and also contain the system error (THE) as indicated by long dash lines. Other information in the figures include the error between the response and the slider (THERR). This piece of information indicates how the slider from the friction model relates to the response. The pound(lb), inch(in), second(sec) system was used through out the simulation process. The unit of torque was lb-in. The unit of angular displacement was in radians (rad). The velocity and acceleration were in rad/sec and rad/sec², respectively. Mass was expressed in lb-sec²/in. The command signal amplitude was 0.2 radians (11.459 °) and the simulation time lasted one second.

B. EFFECT OF FRICTION ON ACCURACY

This section discusses the effect of friction on the system. The system with no friction was simulated and its result was compared with the same system with various friction level. In order to provide a meaningful result, all the simulation variables except μ must remain constant. The control variables K_1 and δ were set at 15 lb-in/rad and 0.05 in, respectively. The value of K_2 was set at 0.5 lb-in-sec/rad. Figures 4.1 through 4.8 are related to this subject. The response of an ideal, balanced, system with no friction, to a step input is shown in Figure 4.1 The rise time¹ of the ideal response was 0.12 seconds with no steady state error. Using the P.D. control scheme with μ equals to 0.1, 0.2, and 0.3; the steady state error increased from 0.00667 to 0.01333 and to 0.02 radians, respectively. The performance of the P.I.D. control action was better. The worst steady state error occurred when μ equal to 0.3 lb-in was only

¹The rise time was taken as the time required for the system to achieve 95% of the steady state value.

0.00424 radians. However, this better accuracy was at the expense of rise time which was 0.24 second. This was twice as slow as in the ideal case. A comparison of position error for different friction level at different gain K_1 was shown in Figure 4.8. This figure also shown some interesting information. It was expected the position error would increase with increase friction at any given set of circumstances. However, the figure indicated that although it was true in general there were cases when an increased μ did not produce a higher error. For example, when K_1 equal to 10 lb-in. rad the position error for μ equal to 0.2 lb-in had a higher position error (2.5 milli-radians) compared to 0.84 milli-radians for μ equal to 0.3 lb-in. This was due to the nonlinearity of the system. A particular K_2 combined with a suitable K_1 and δ would produce a better error.

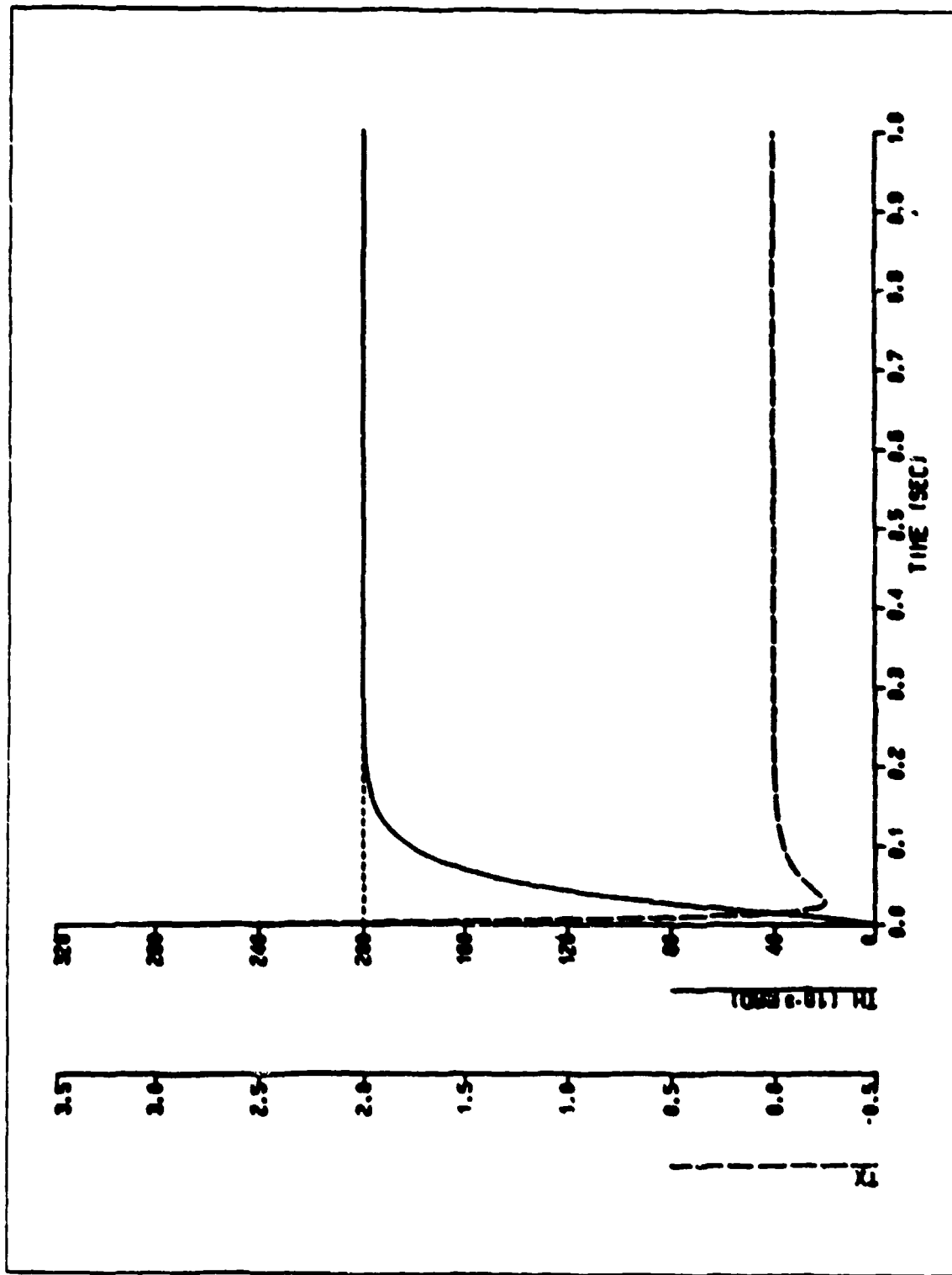


Figure 4.1 Balanced System, PD Control. No Friction

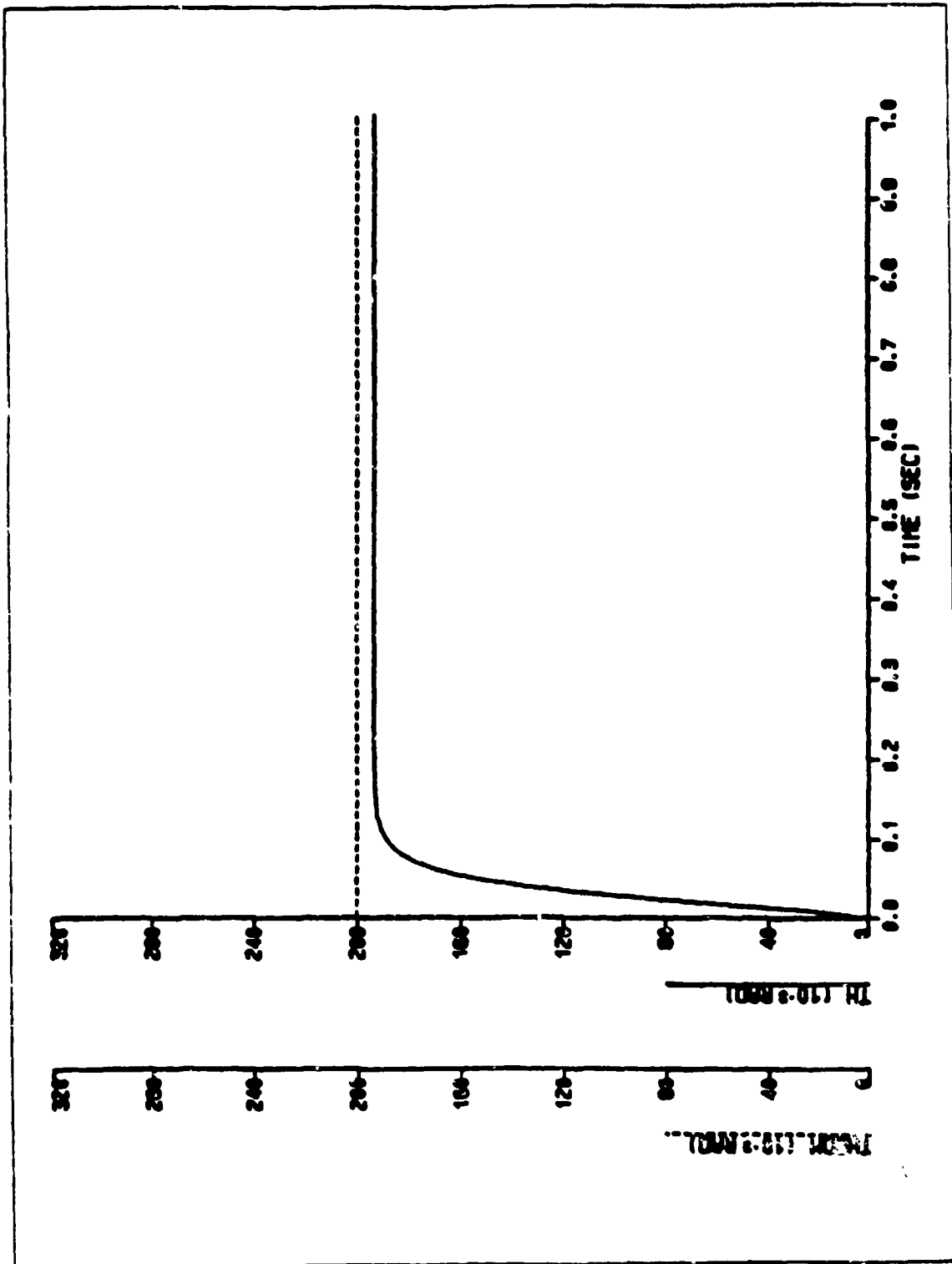


Figure 4.2 $\mu = 0.1$, $K_1 = 15.0$, $K_2 = 0.5$, $\delta = 0.05$

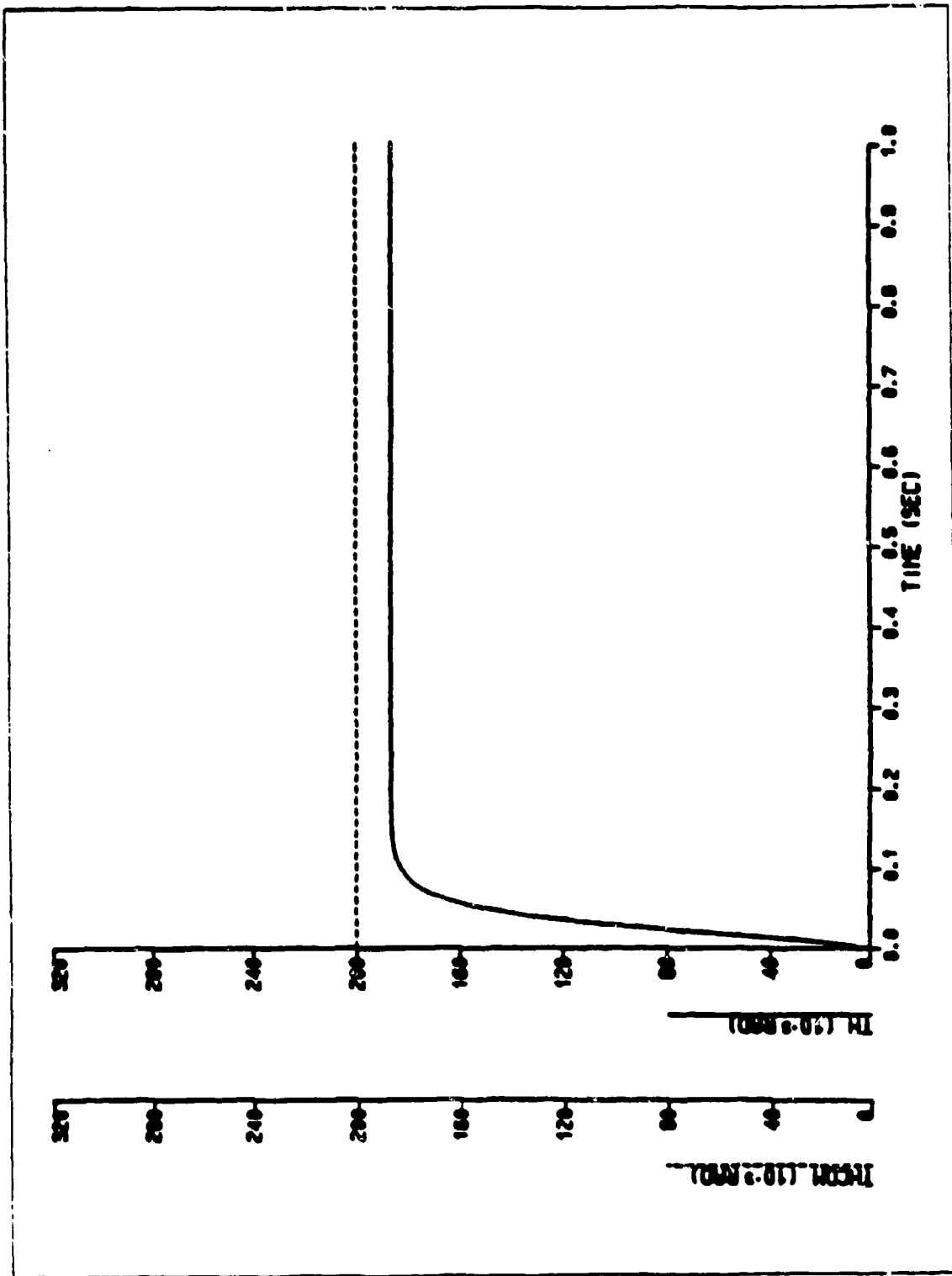


Figure 4.3 $\mu = 0.2$, $K_1 = 15.0$, $K_2 = 0.5$, $\delta = 0.05$

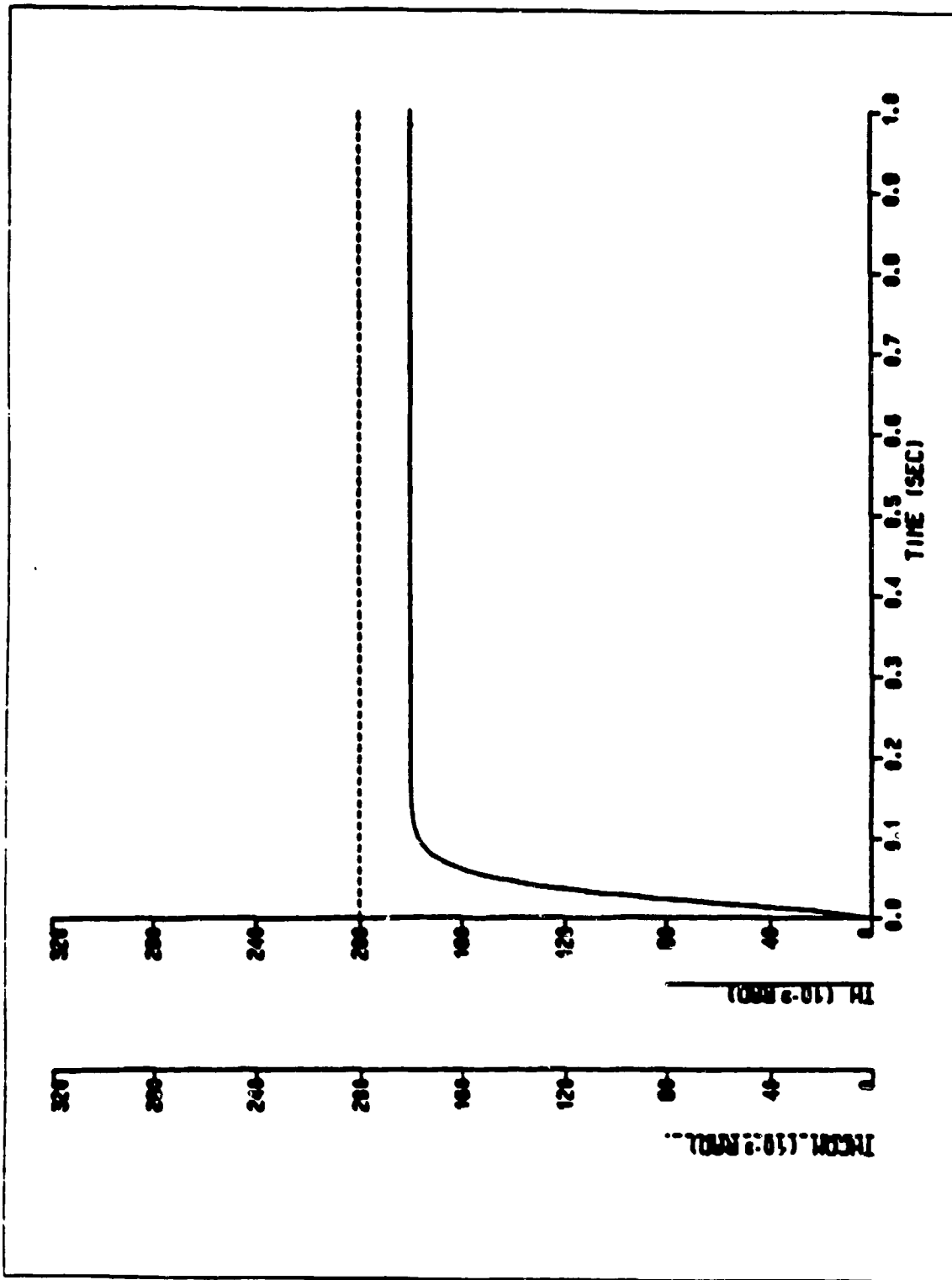


Figure 4.4 $\mu = 0.3$, $K_1 = 15.0$, $K_2 = 0.5$, $\delta = 0.05$

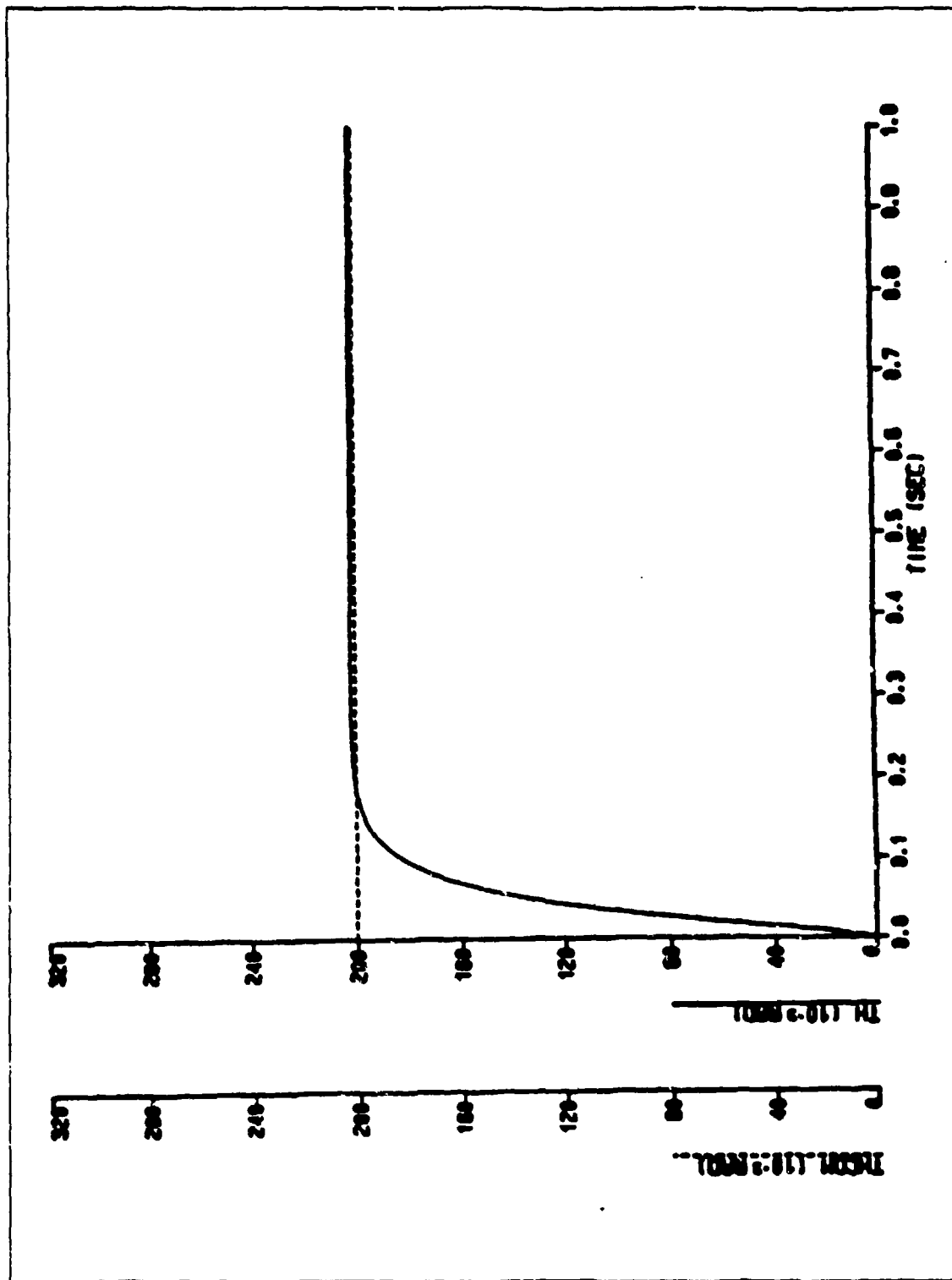


Figure 4.5 $\mu = 0.1$, $K_1 = 15.0$, $K_2 = 0.5$, $\delta = 0.05$, PID Control $T_i = 1.0$

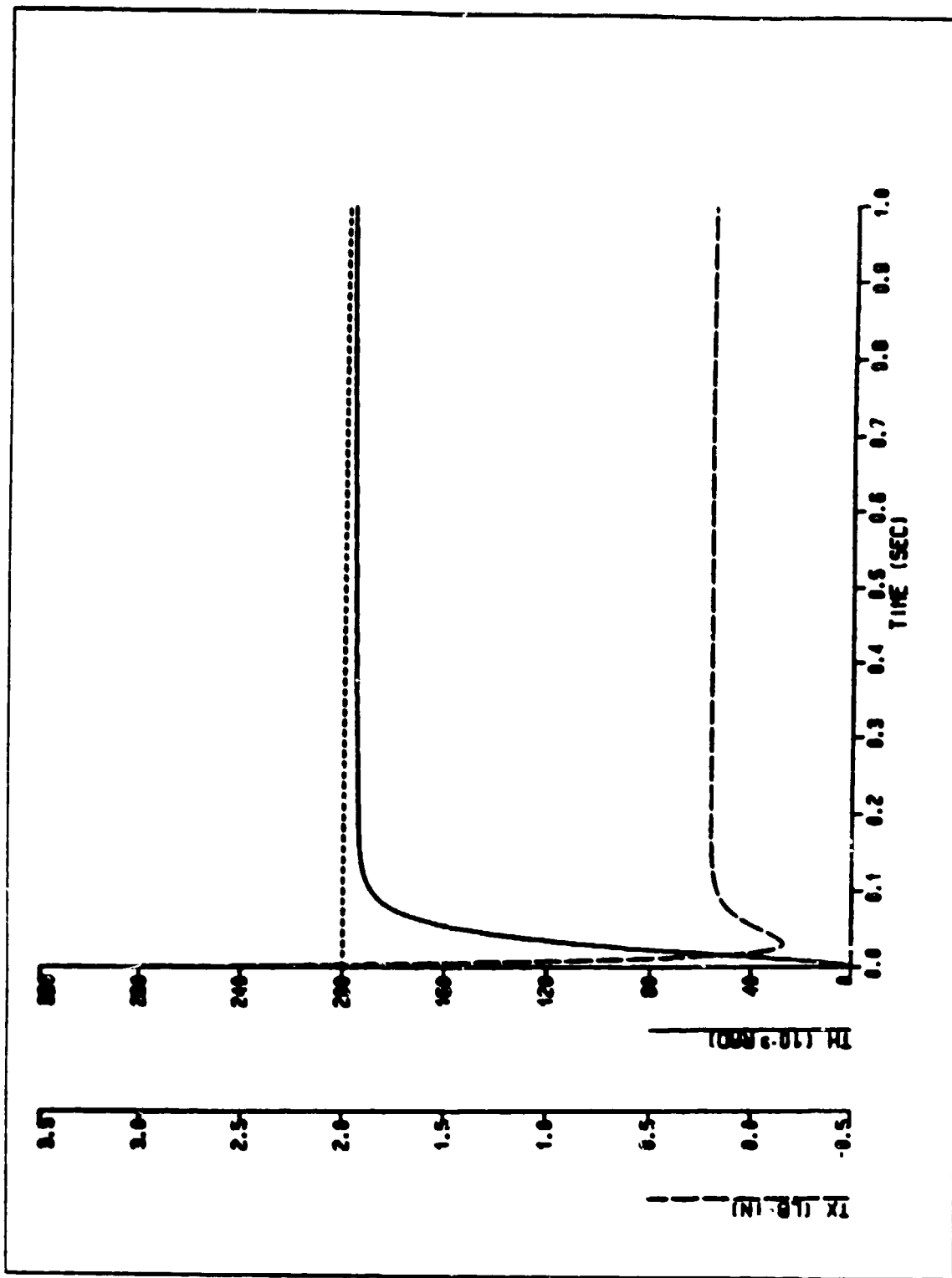


Figure 4.6 $\mu = 0.2$, $K_1 = 15.0$, $K_2 = 0.5$, $\delta = 0.05$, PID Control $T_i = 1.0$

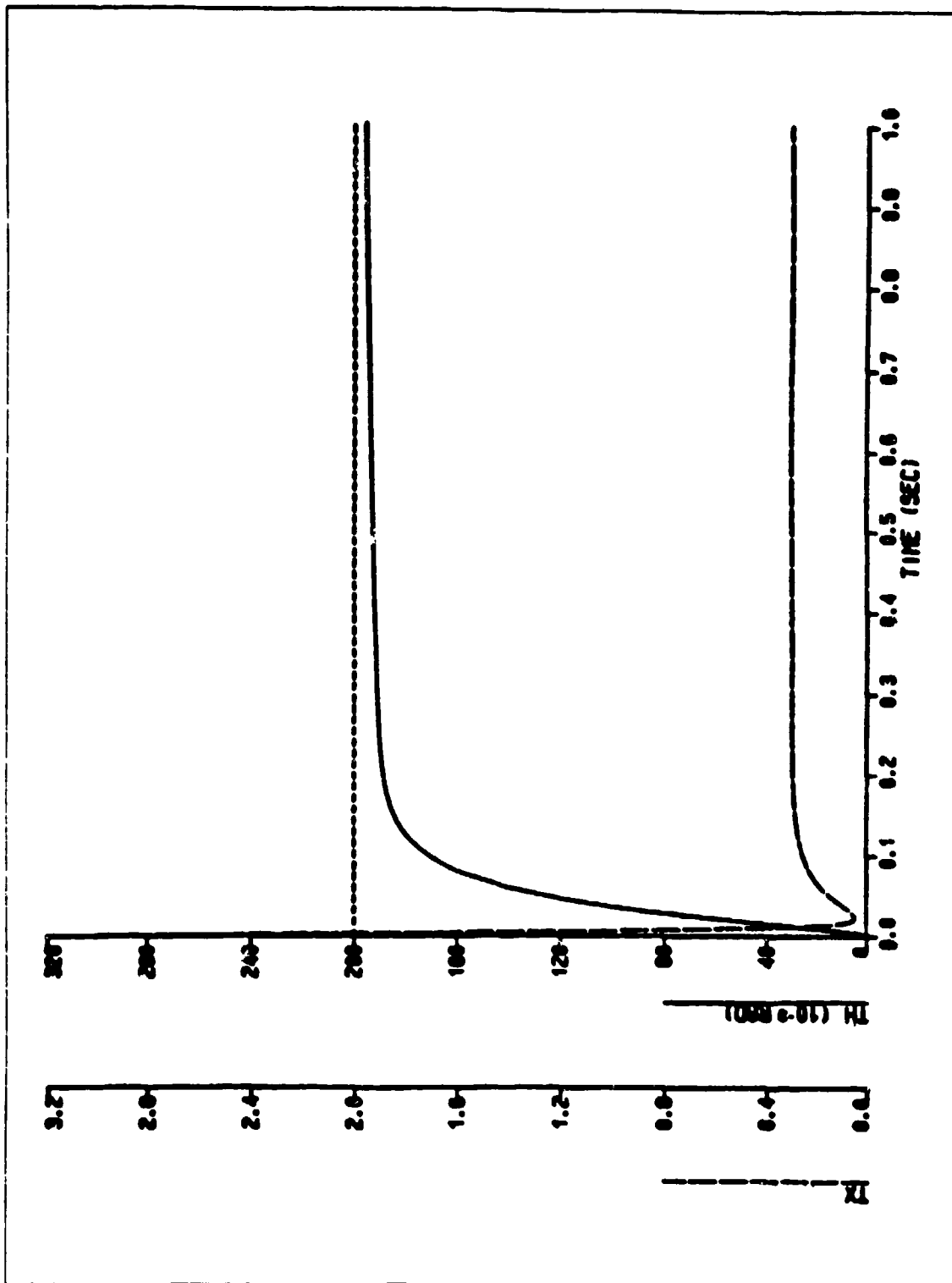


Figure 4.7 $\mu = 0.3$, $K_1 = 15.0$, $K_2 = 0.5$, $\delta = 0.05$, PID Control $T_i = 1.0$

C. EFFECT OF THE K_1

The usual method of minimizing the influence of disturbance forces such as the frictional load is to increase the feedback gain, K_1 , so that system "stiffness" is increased. However, while this works with clean signals, the effects of sensor noise provides a limit on the useful range of K_1 . The deliverable torque by the motor also limits the values of K_1 . Figures 4.9 through 4.14 provide graphical results to different K_1 s. A high K_1 value drastically reduces the position error of the system as shown in Figure 4.8. The steady state error decreased from 73.88% to 10% when K_1 increased from 2 lb-in./rad to 15 lb-in./rad. Like wise, the positional error to a sinusoidal input decreased from 0.12559 radians to 0.01764 radians when K_1 increased from 15 lb-in./rad to 1000 lb-in./rad. The response followed the command signal rather well at the higher K_1 value with a phase shift of less than 0.01 seconds. The torque delivered to the system was also higher, an increase of 65%, compared with the lower K_1 value of 15 lb-in./rad.

D. EFFECT OF SPRING CONSTANT

Figures 4.15 through 4.20 shown the effect of spring stiffness to position error. The spring constant, δ , appeared to have little effect on the steady state error but it did affect the torque delivery to the platform. A very stiff spring, small δ , required more torque than a softer spring as expected. Indeed, it was shown in Figures 4.15 and 4.16. However, this logic did not work in Figure 4.17. The torque delivery in this case was higher. The effect on a sinusoidal input was a little different. The stiffer spring performed poorer than the softer spring. The maximum error was 0.18527 radians for the stiff spring and 0.14129 radians for the softer spring. However, the softer spring followed the signal a little better than the stiff spring. The time lag was 0.07 second for the stiff spring and 0.04 second for the soft spring. Compares with the ideal case where there was no friction, the maximum error was 0.12092 radians with a time lag of 0.04 seconds as shown in Figure 4.18.

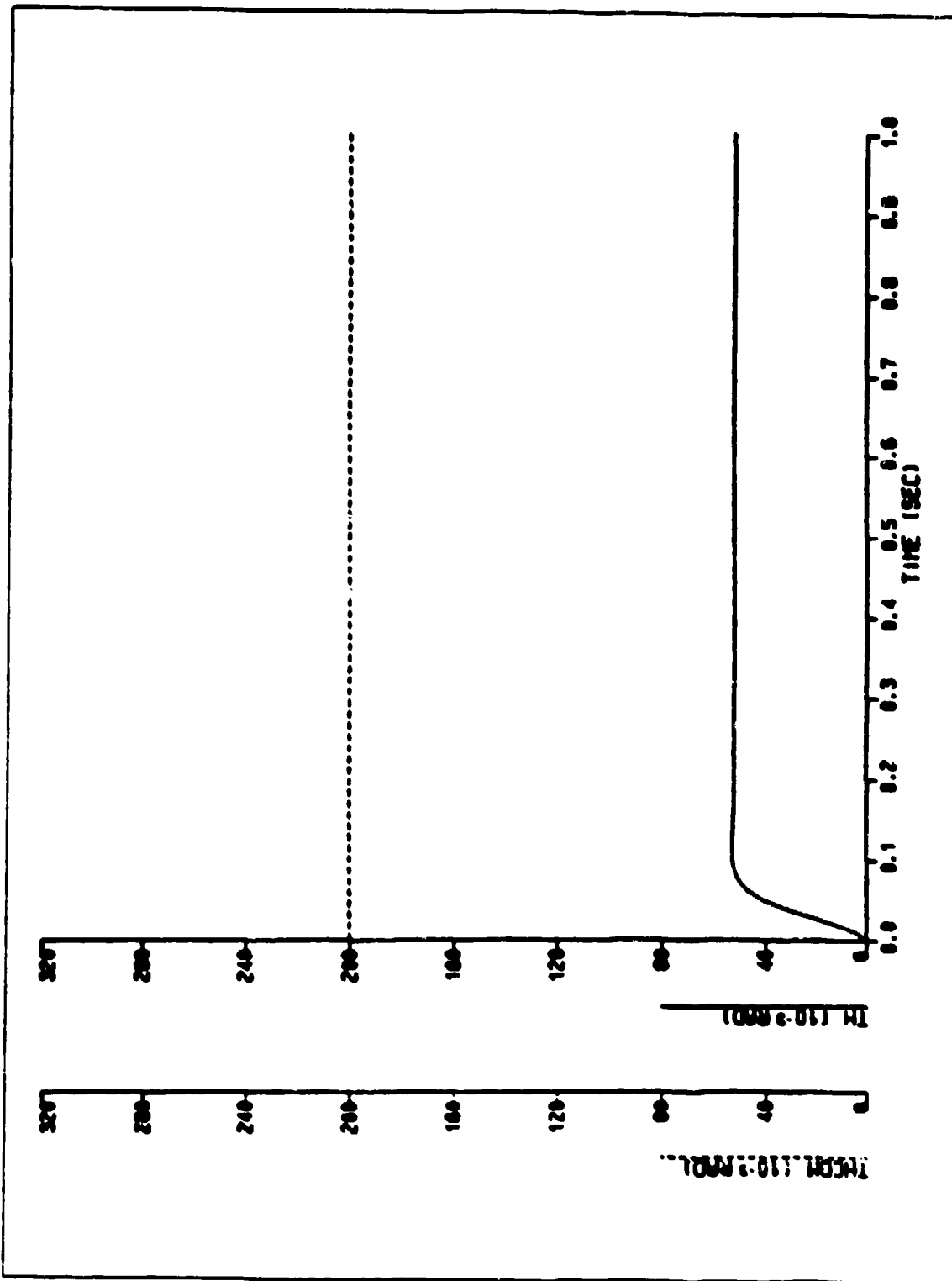


Figure 4.9 $\mu = 0.3$, $K_1 = 2.0$, $\delta = 0.05$

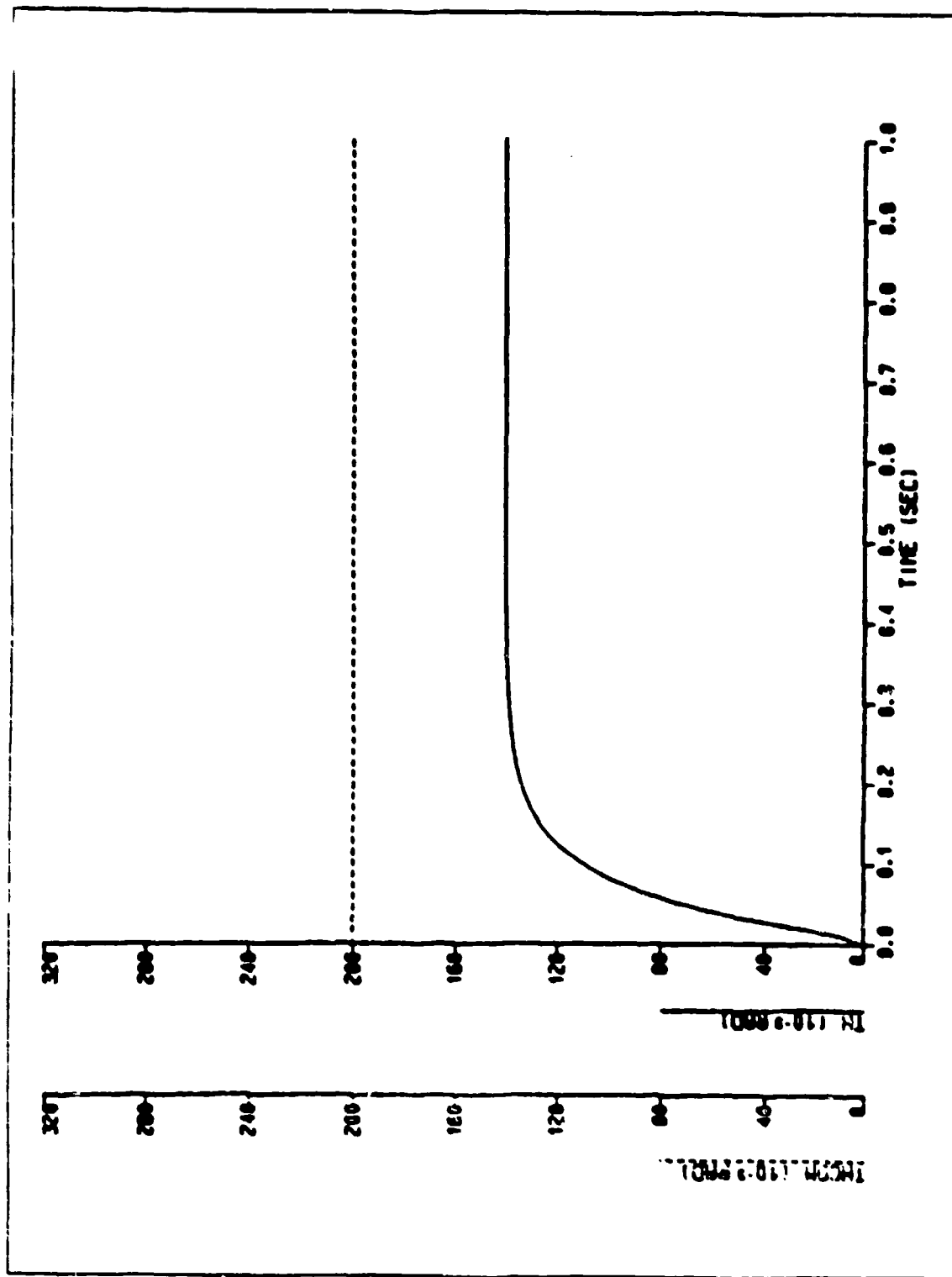


Figure 4.10 $\mu = 0.3$, $K_1 = 5.0$, $\delta = 0.05$

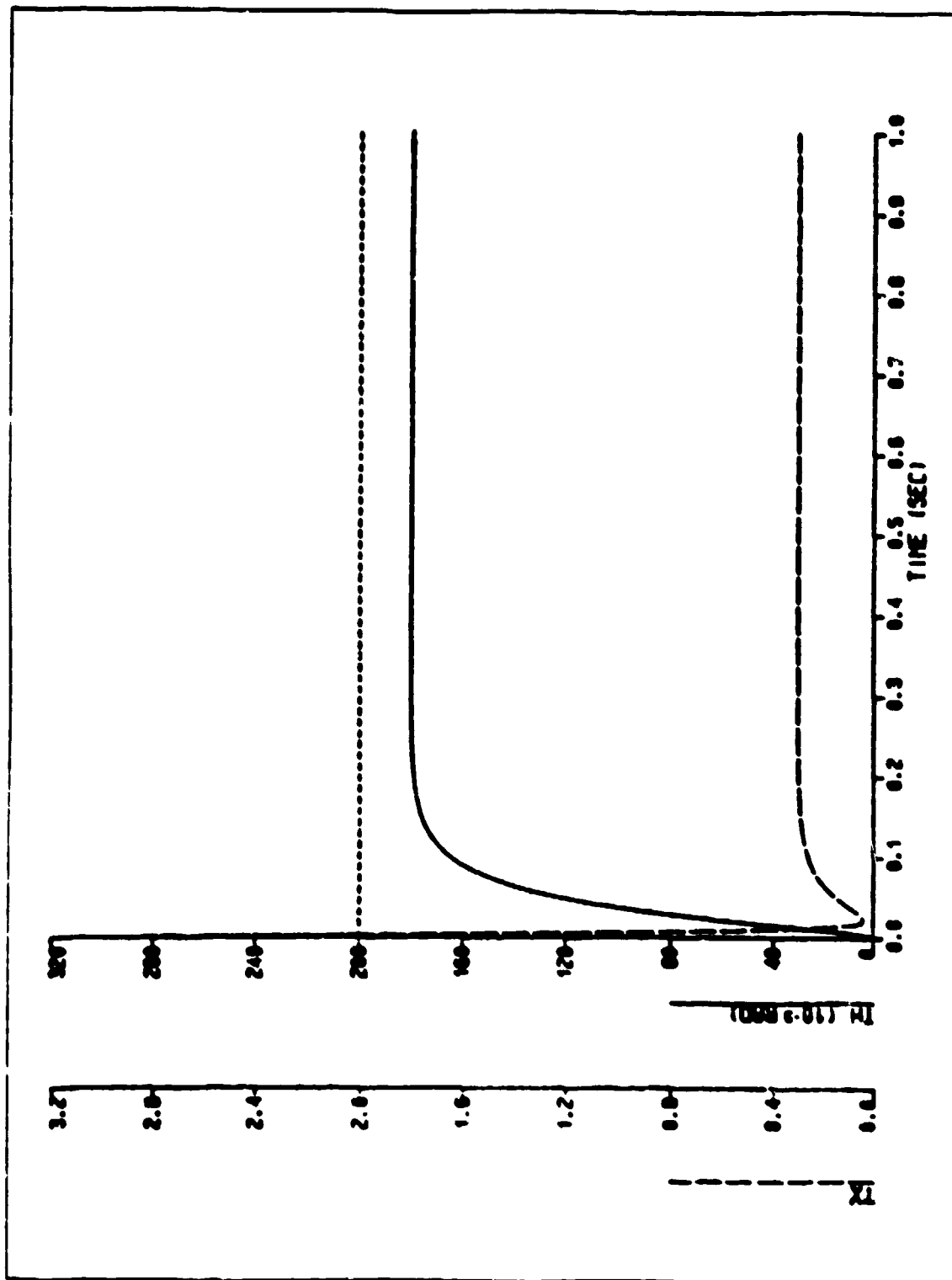


Figure 4.11 $\mu = 0.3$, $K_1 = 15.0$, $\delta = 0.05$

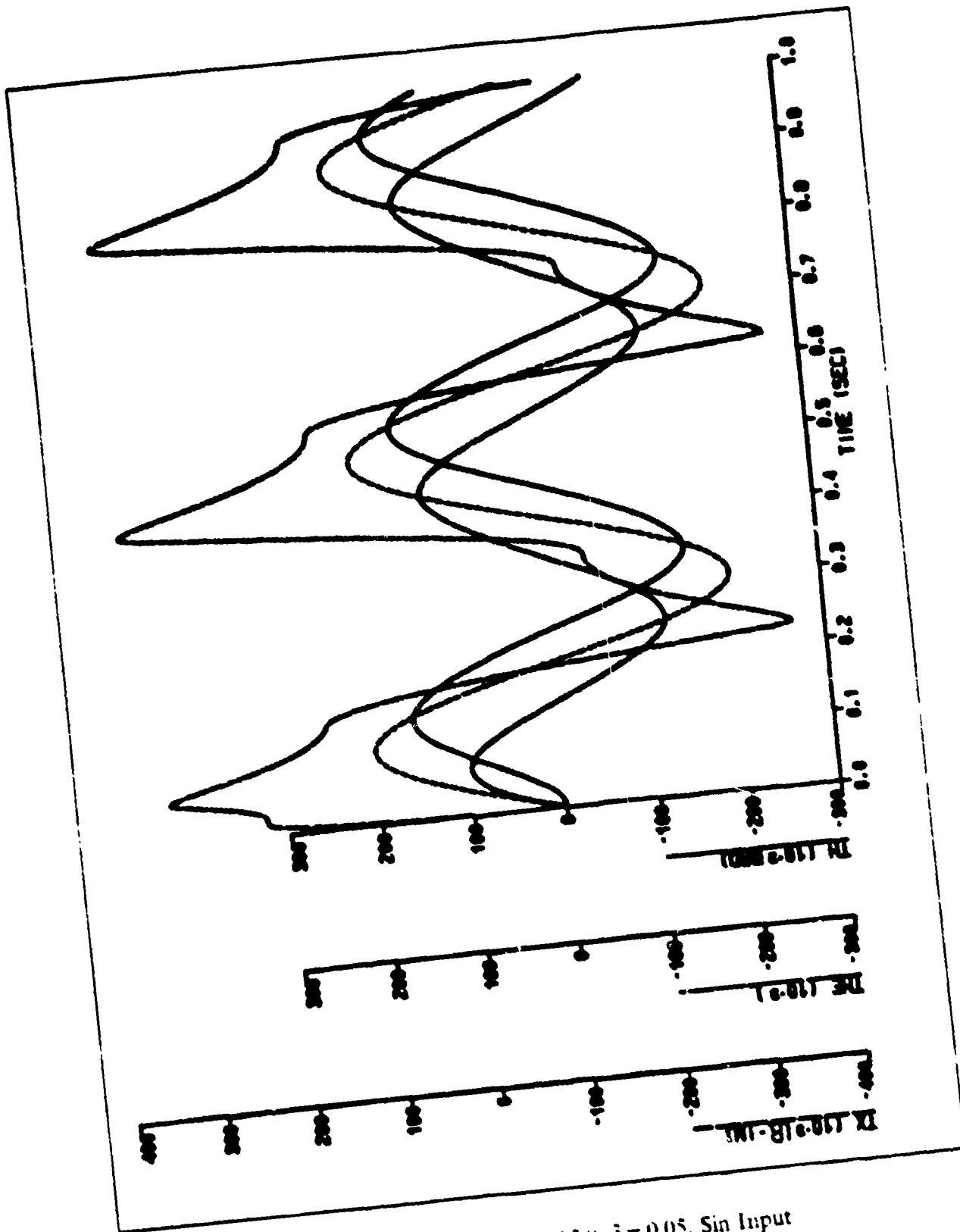


Figure 4.12 $\mu = 0.3$, $K_1 = 15.0$, $\delta = 0.05$, Sin Input

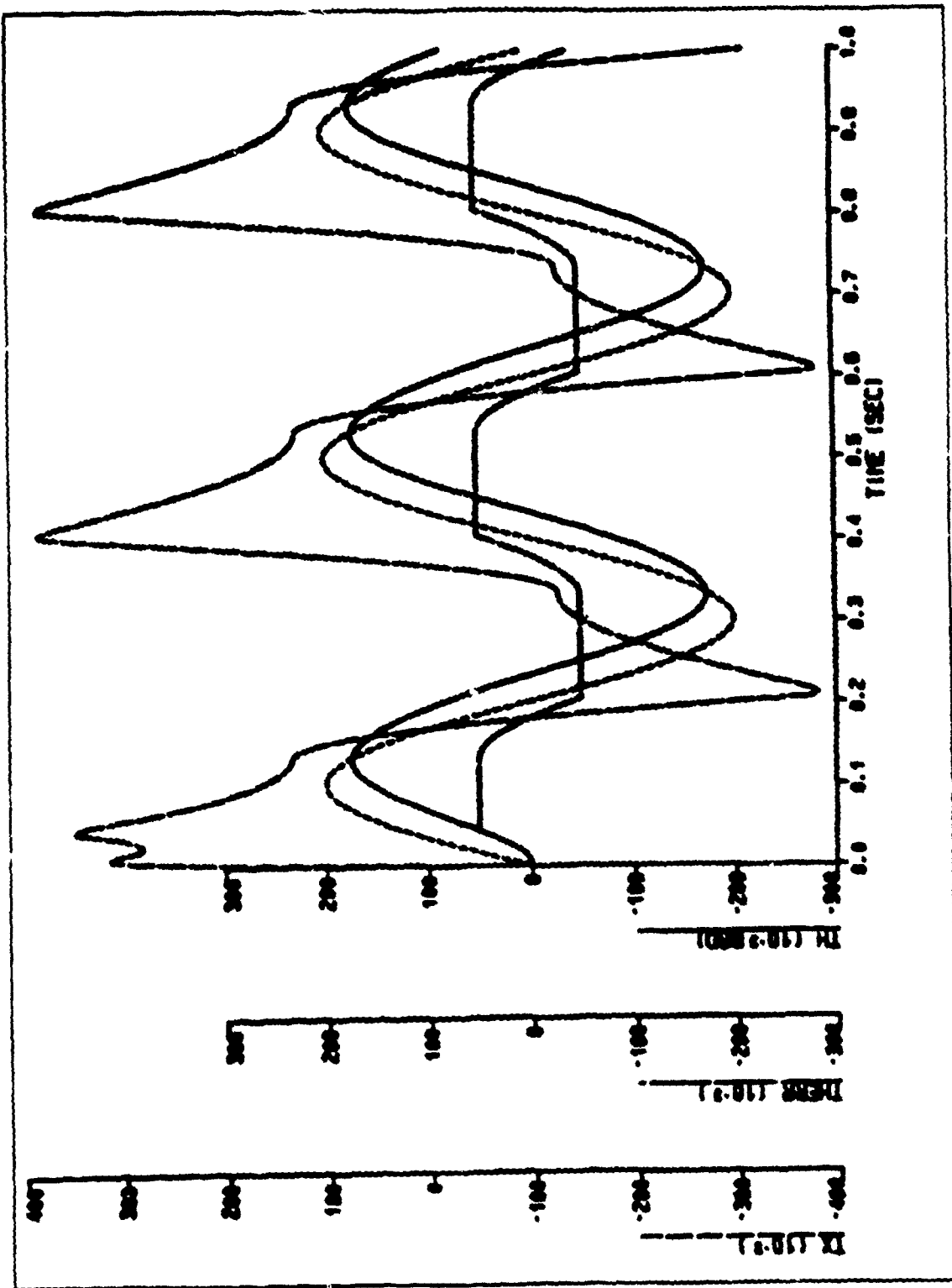


Figure 4.13 $\mu=0.3$, $K_1=30.0$, $\delta=0.05$, Sin Input

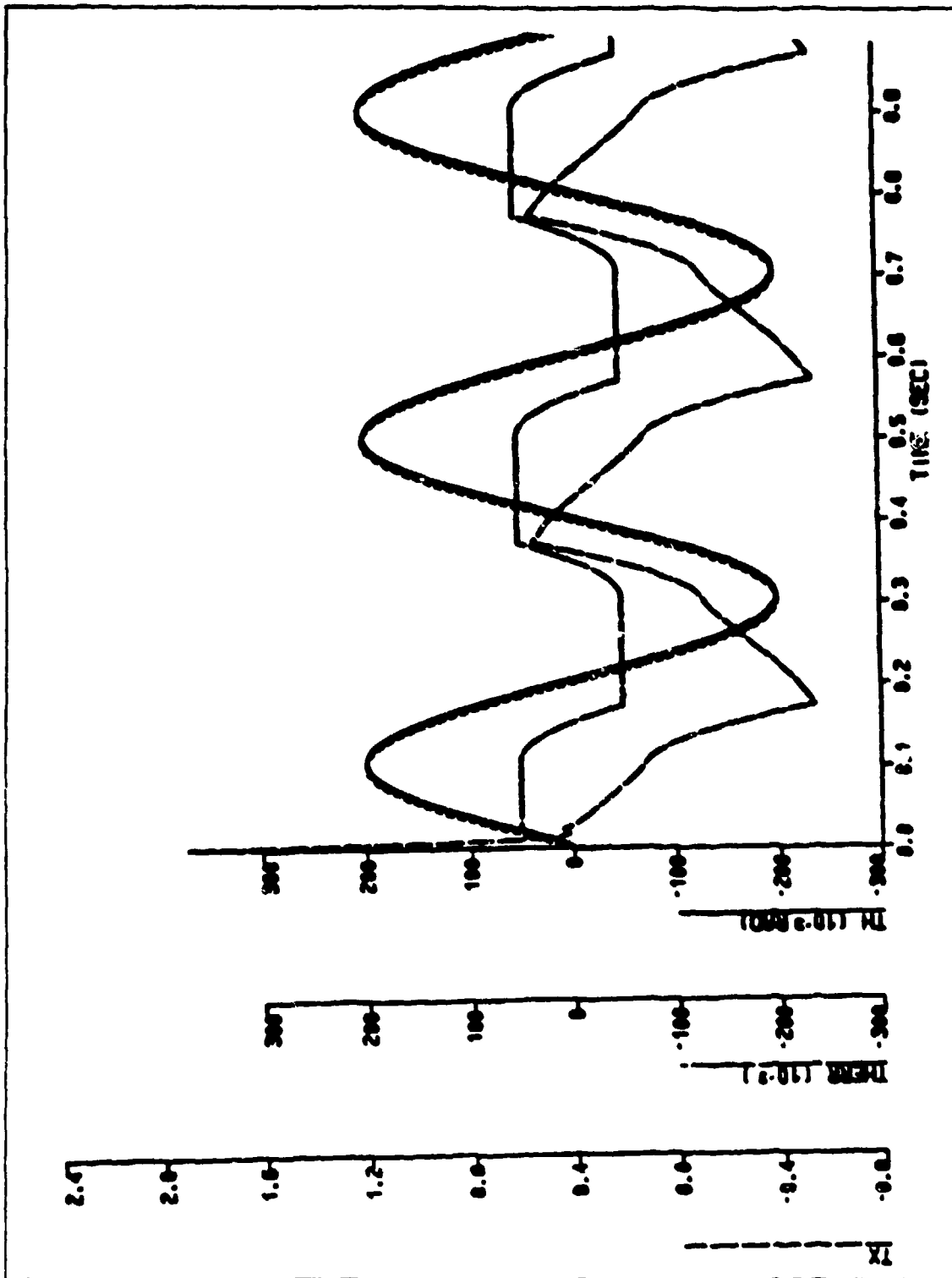


Figure 4.14 $\mu = 0.3$, $K_1 = 1000.0$, $\delta = 0.05$, Sin Input

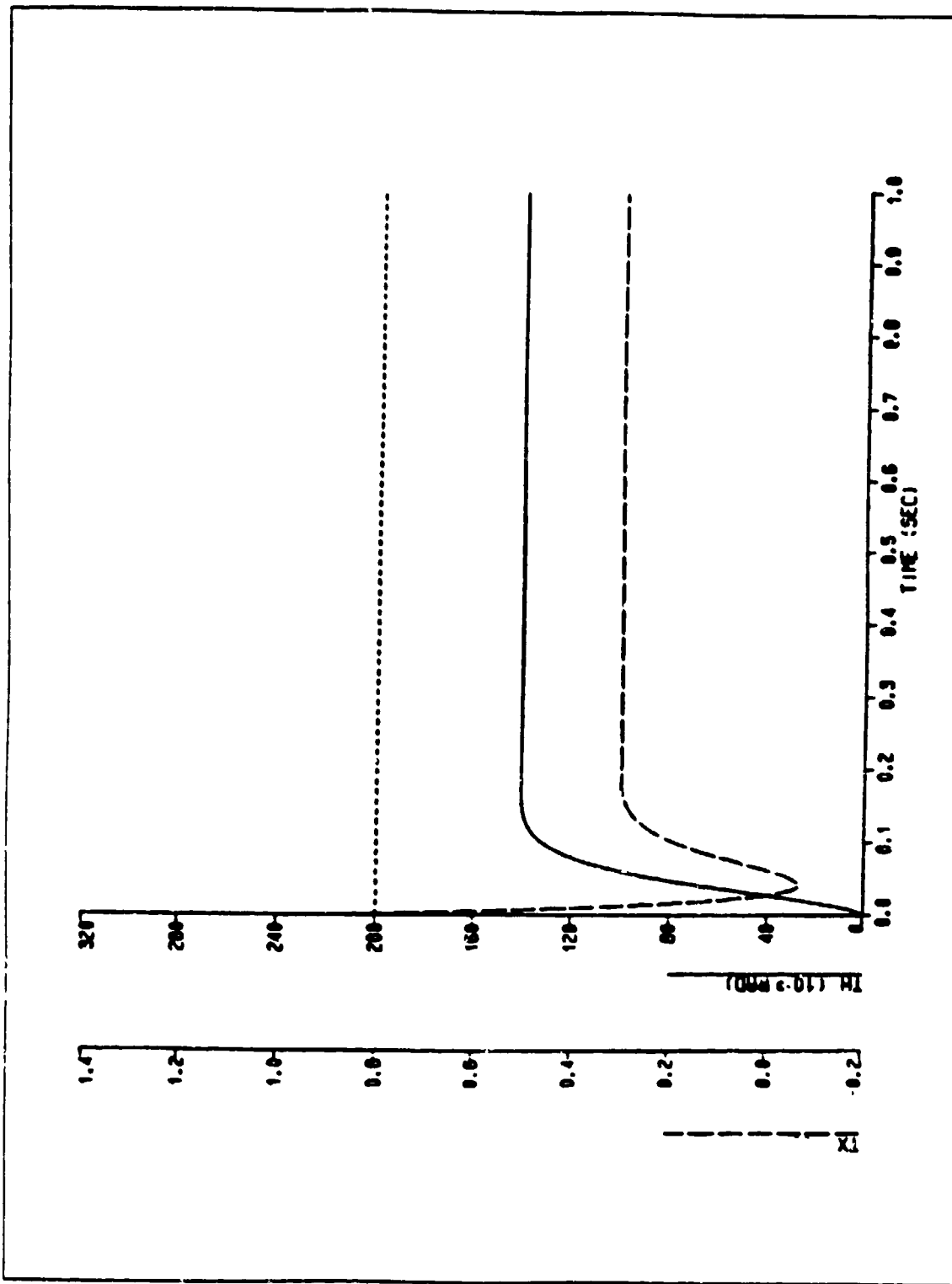


Figure 4.15 $\mu = 0.3$, $K_1 = 5.0$, $\delta = 0.001$

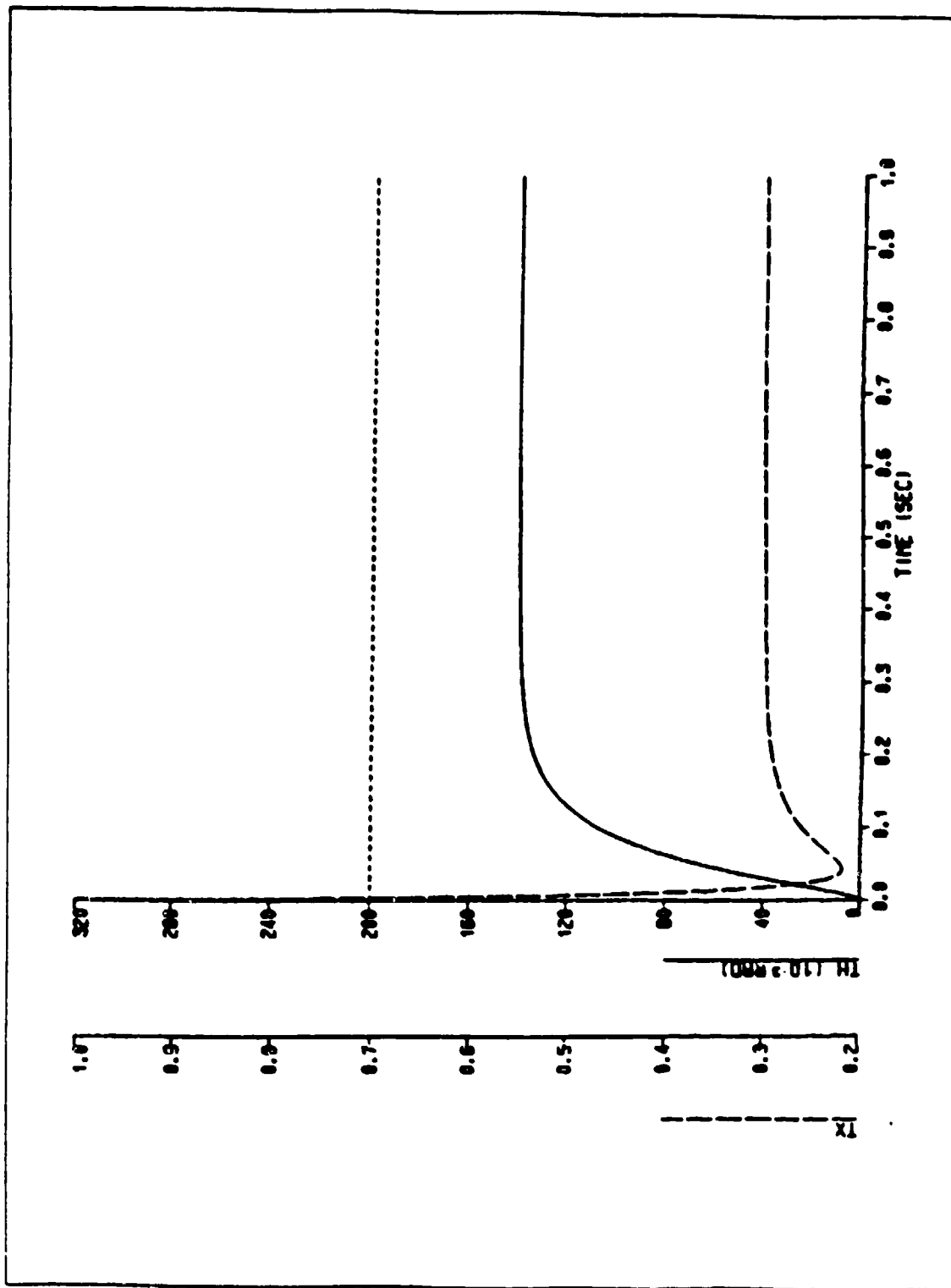


Figure 4.16 $\mu = 0.3$, $K_1 = 5.0$, $\delta = 0.01$

E. EFFECT OF INTEGRAL GAIN TIME CONSTANT

The benefit of an integral action was demonstrated in Section B. This section studied the effect of the integral time constant. When the time constant was set to unity (Figure 4.5), the response overshoot by 0.00188 radians (0.94%) and then settled back to 0.20104 radians at the end of one second. With the time constant increases to 2 and 3 seconds, the response did not exhibit any overshoot as shown in Figures 4.21 and 4.22. It did indicate that as the time constant increases, the steady state error also increases, even though the increase was small.

F. EFFECT OF G_1

This section as well as the next section focuses on the control variables G_1 and μ prediction on the accuracy of the seeker using the model-reference technique. It was shown in previous sections that the sinusoidal input produced an error due to the inability of the seeker to track accurately, even in the case where friction was not present. This was mainly due to the inability of the P.D. or P.I.D. control action's failure to correct the inertia effect of the platform in a timely manner. The effect of G_1 was illustrated in Figures 4.23 through 4.25. In Figure 4.23, the maximum error was 0.09086 radians and a time lag of 0.03 seconds with K_1 and G_1 both equal to 30. It is interesting to observe that the performance did not degrade even though the value of K_1 was reduced by half provided the value of G_1 was high. In fact, the performance can be improved by increasing G_1 . As shown in Figure 4.24 and 4.25, both the maximum error and time lag were drastically reduced to 0.02417 rad and 0.01 rad as G_1 increases to 500 and 3000, respectively. The amount of time lag also cut by a third to less than 0.01 second. Although the value of G_1 was arbitrary, it was not without bound. The maximum usable value depends on the size of the torque motor.

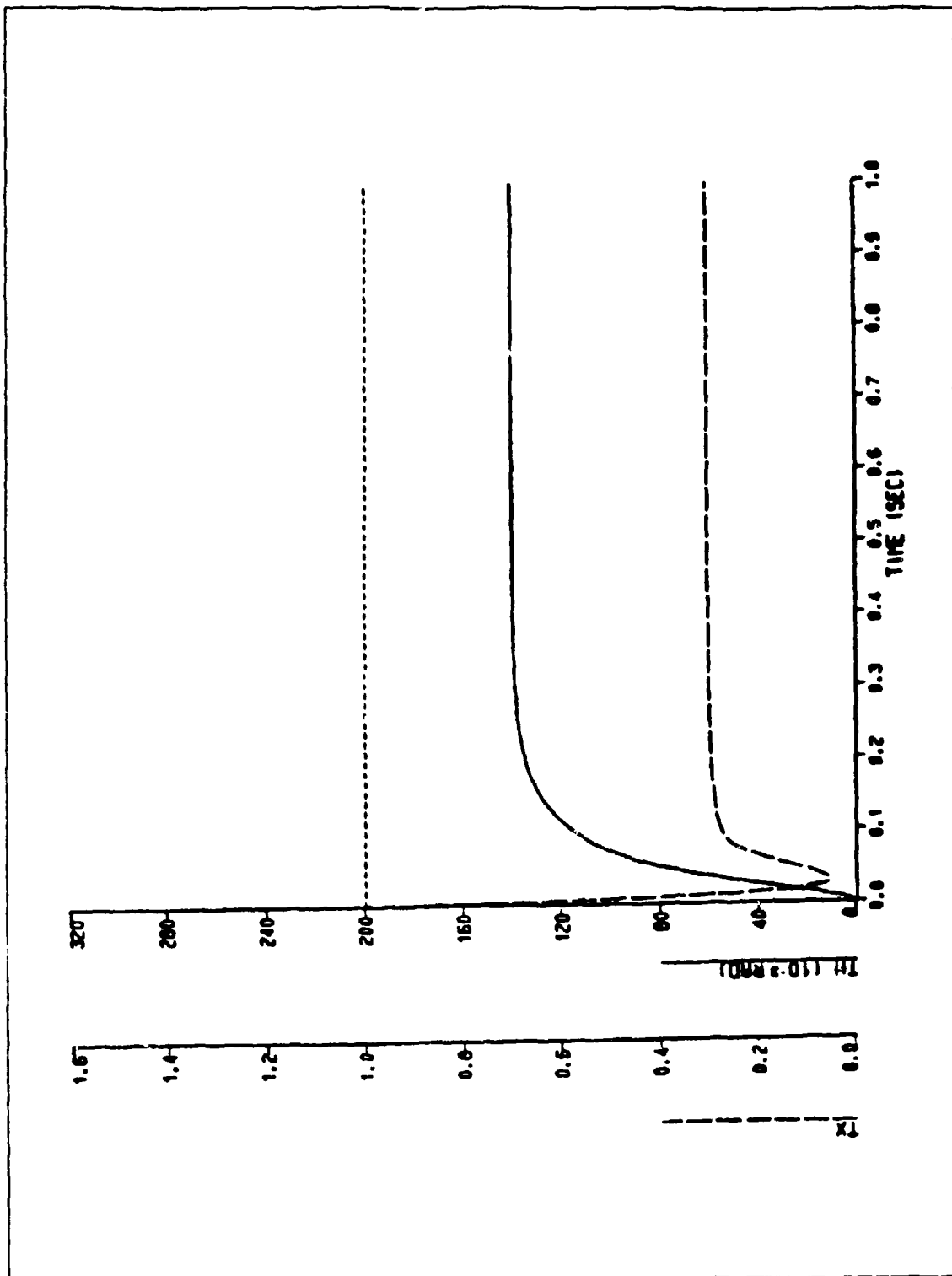


Figure 4.17 $\mu = 0.3$, $K_1 = 5.0$, $\delta = 0.1$

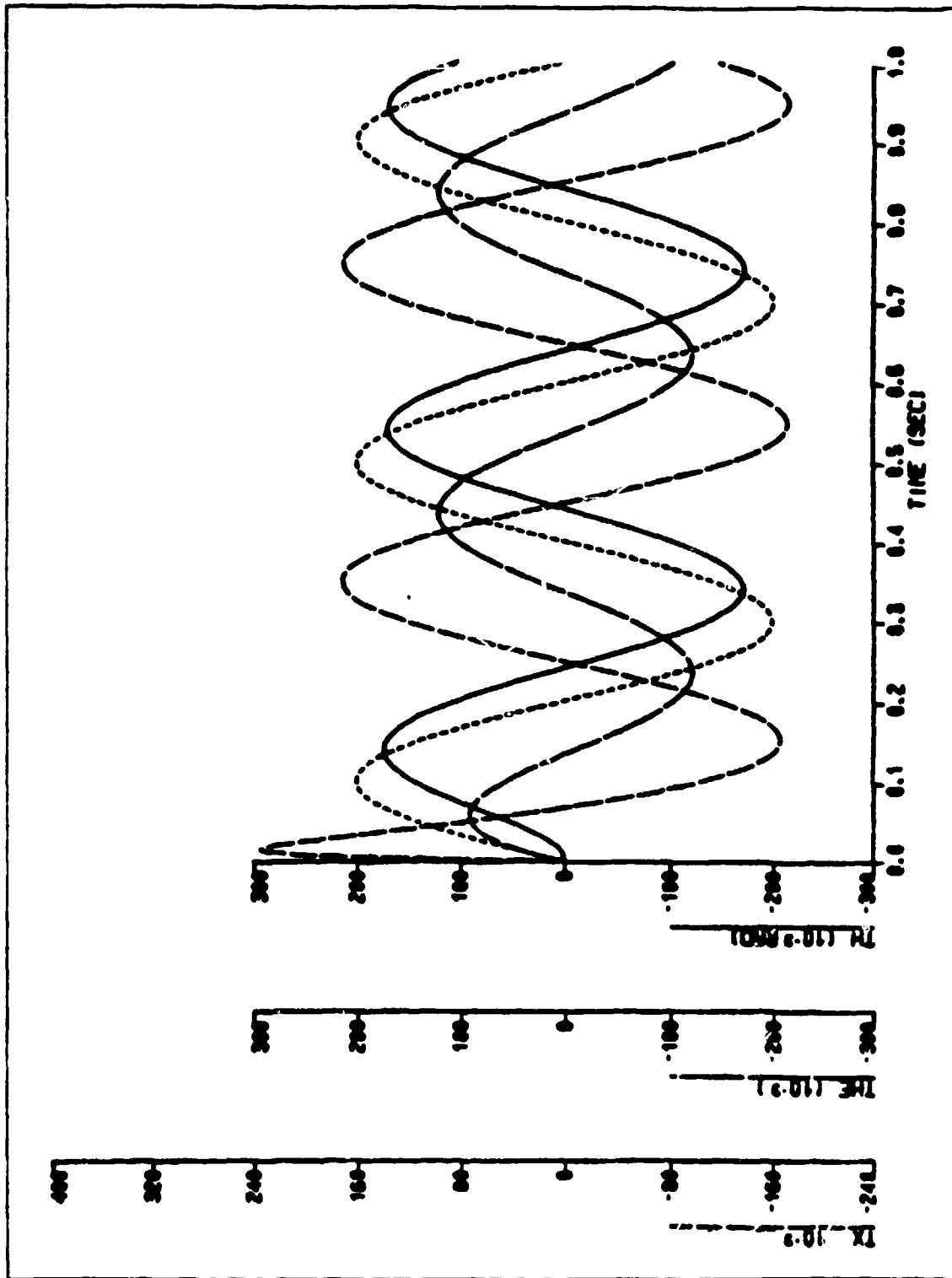


Figure 4.18 Balanced System, PD Control, No Friction, Sin Input

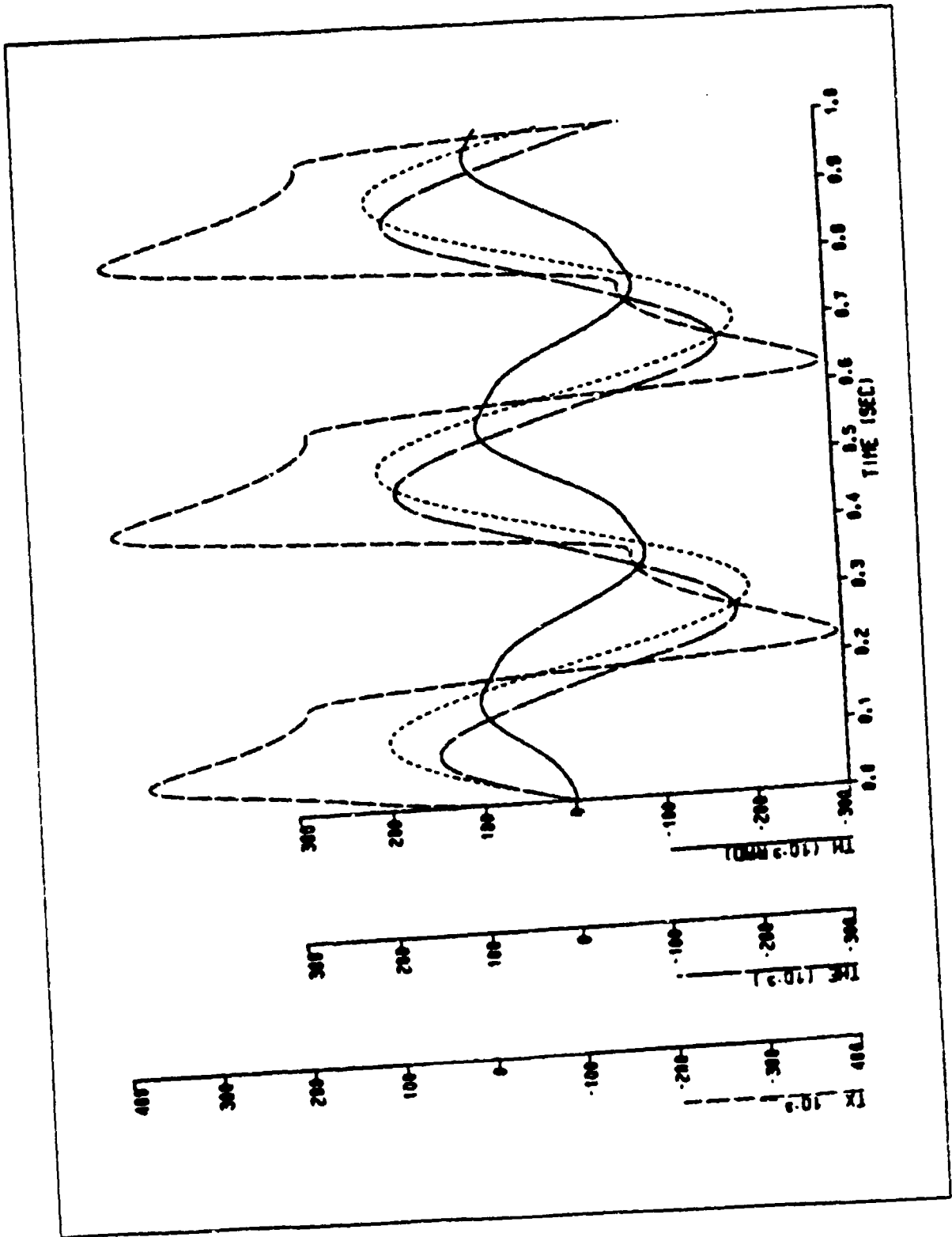


Figure 4.19 $\mu = 0.3$, $K_1 = 5.0$, $\delta = 0.01$, Sin Input

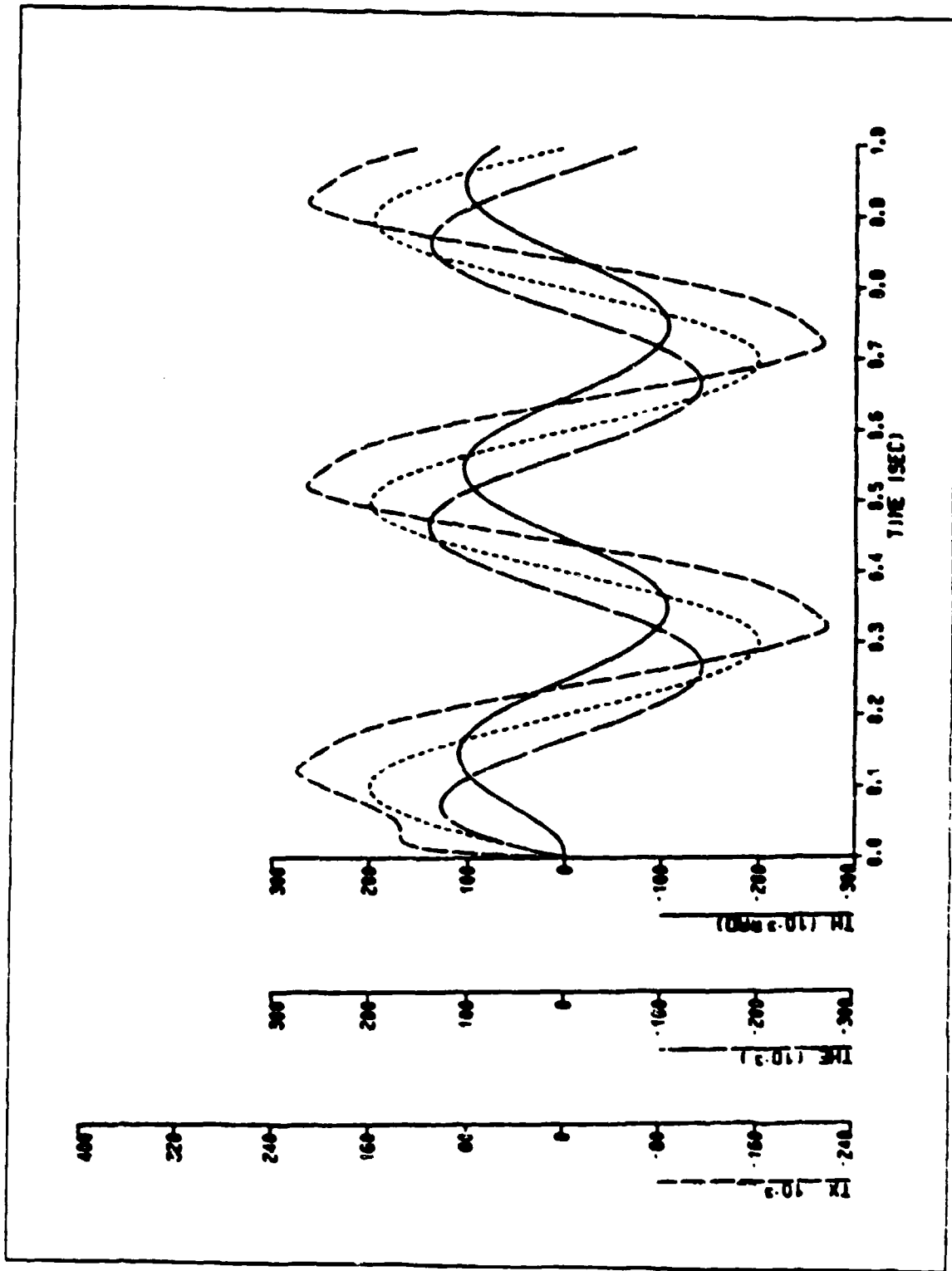


Figure 4.20 $\mu = 0.3$, $K_1 = 5.0$, $\delta = 0.1$. Sin Input

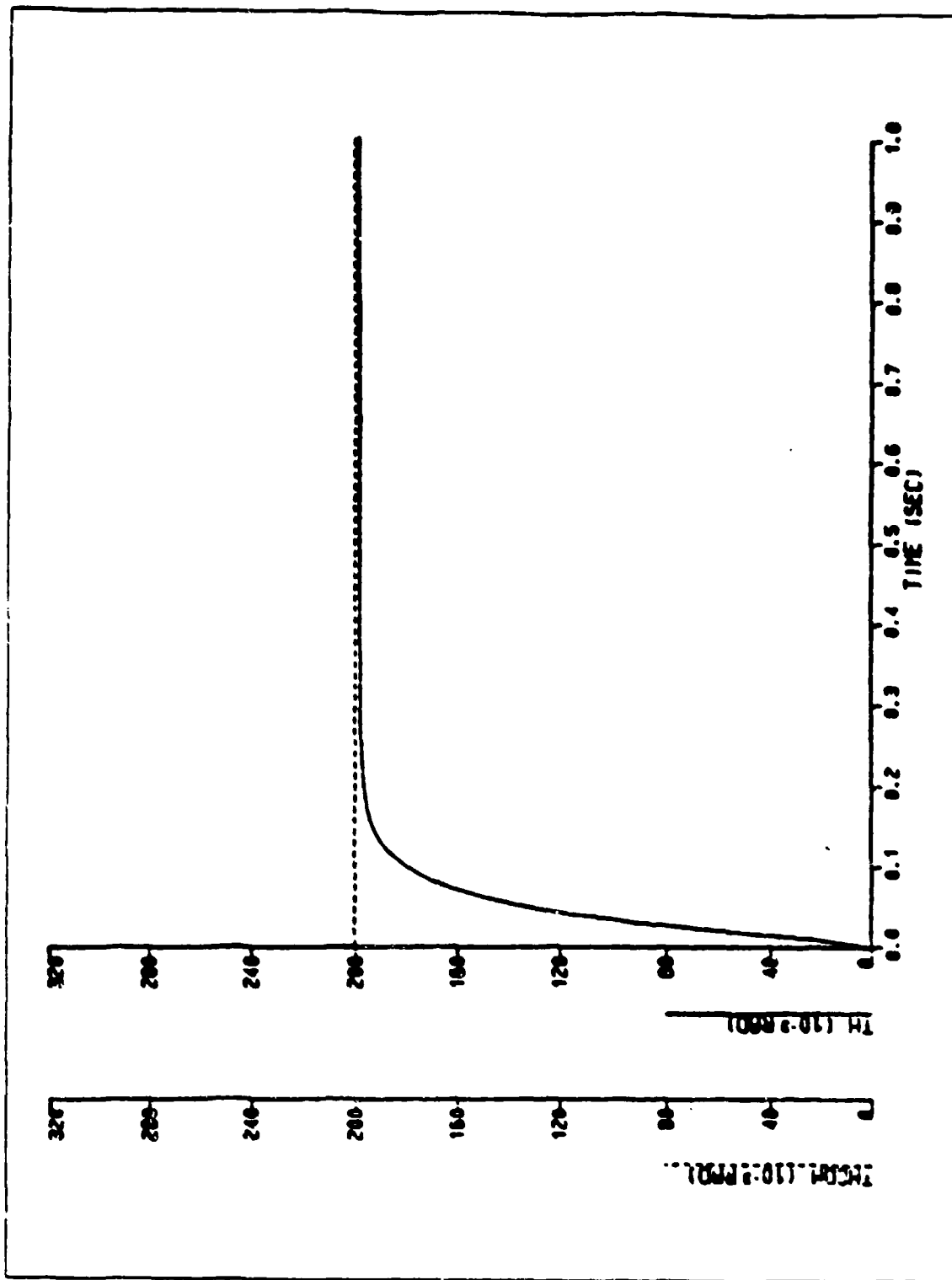


Figure 4.21 $K_1 = 15.0$, $\delta = 0.05$, PID Control, $T_i = 2$

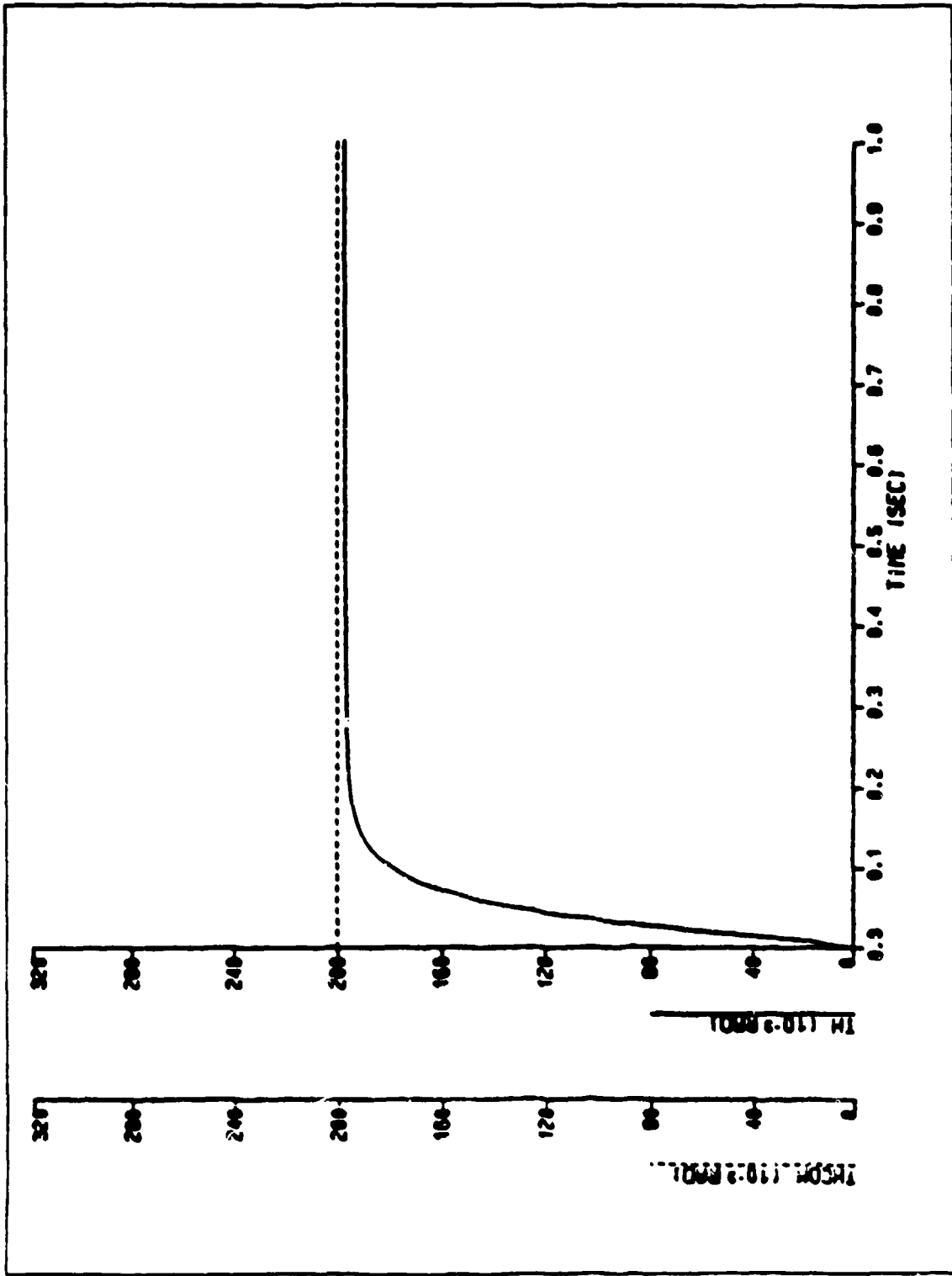


Figure 4.22 $\mu = 0.1$, $K_1 = 15.0$, $\delta = 0.05$, PID Control, $T_1 = 3$

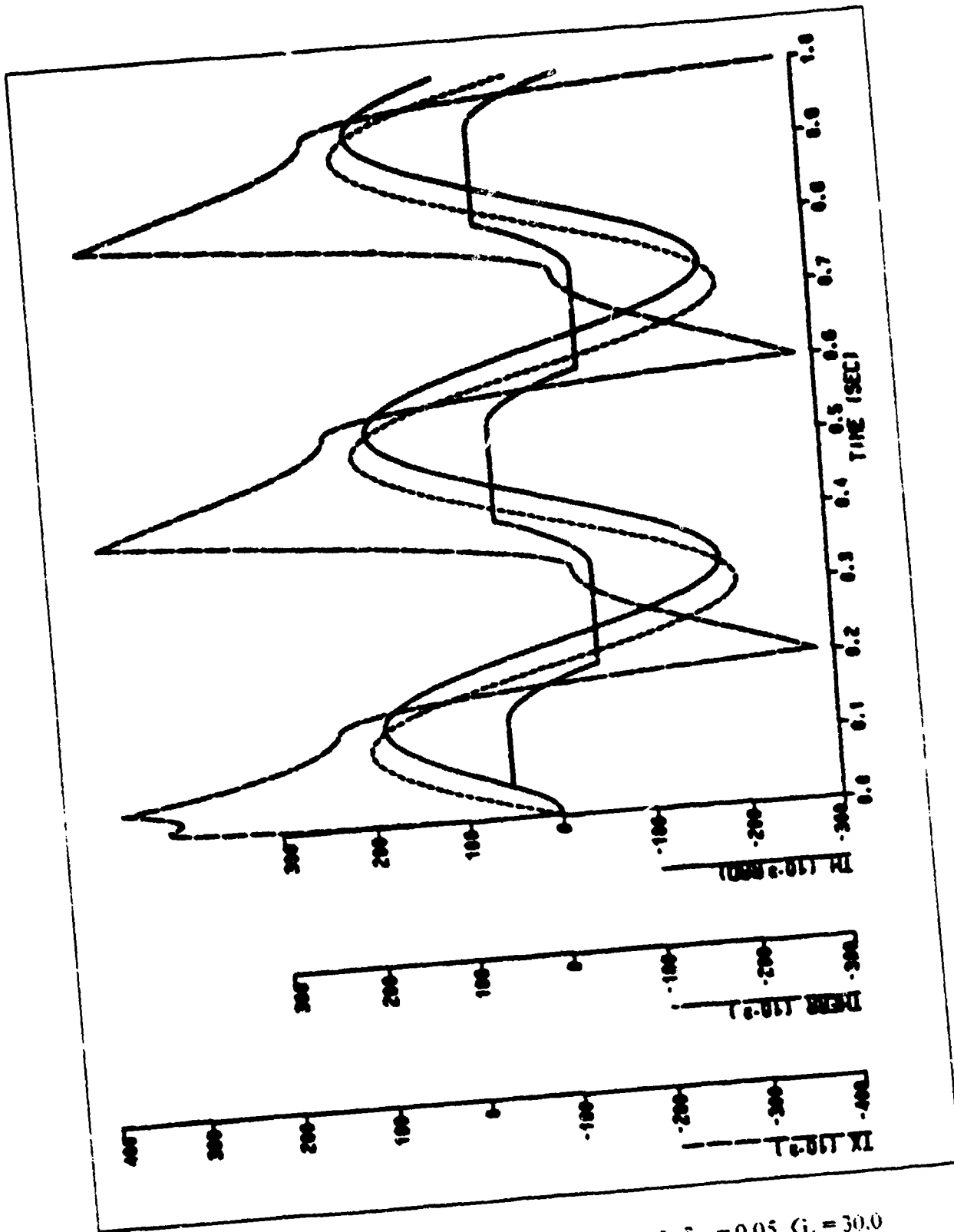


Figure 4.23 $\mu = 0.3$, $K_1 = 30.0$, $\delta = 0.05$, $\mu_m = 0.3$, $\delta_m = 0.05$, $G_1 = 30.0$

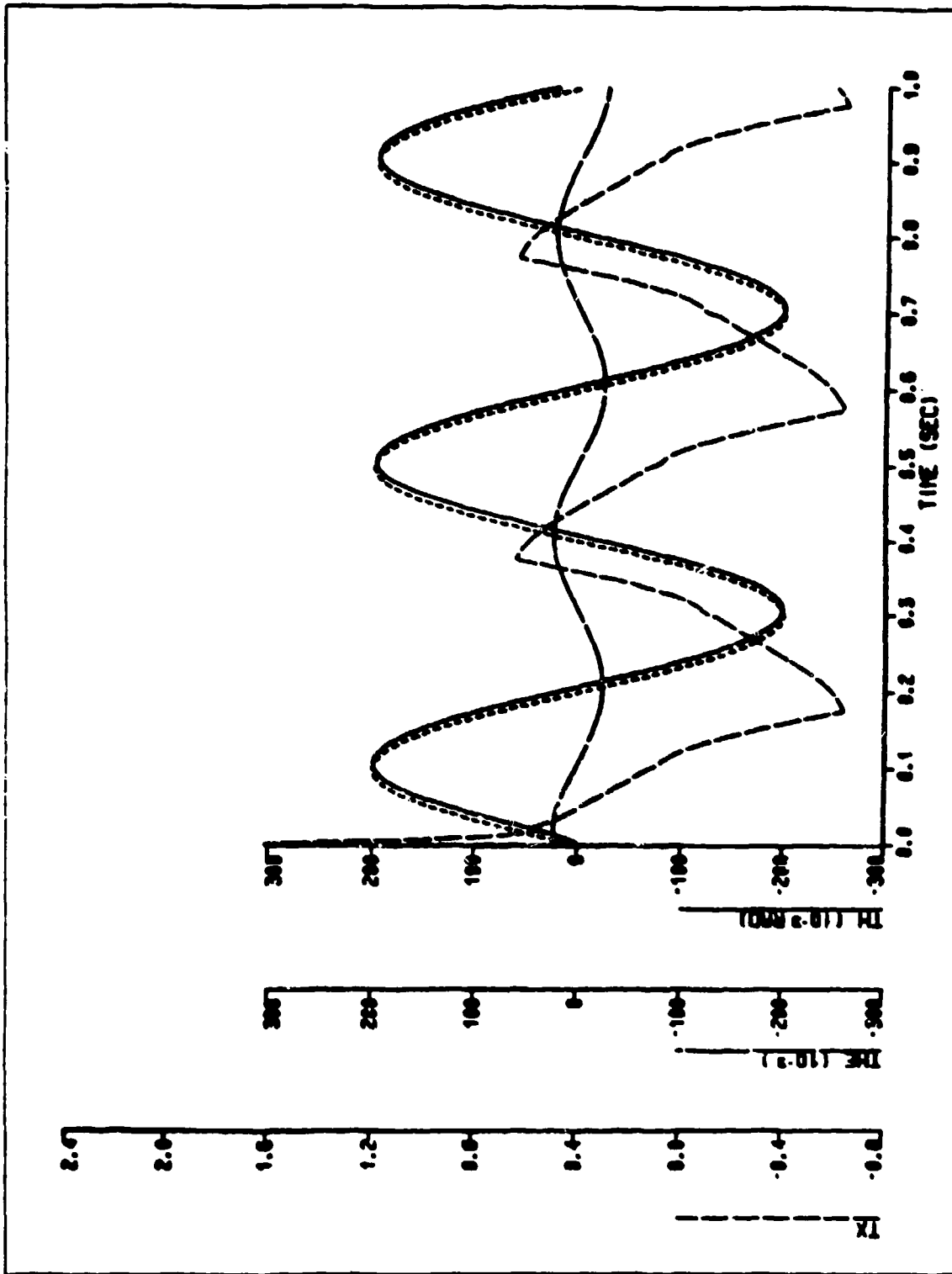


Figure 4.24 $\mu = 0.3$, $K_1 = 30.0$, $\delta = 0.05$, $\mu_m = 0.3$, $\delta_m = 0.05$, $G_1 = 500.0$

G. EFFECT OF μ PREDICTION ERROR

The main advantage of the model-reference control scheme is its ability to predict the response of the system using an ideal model. Figures 4.26 through 4.29 study the sensitivity to an erroneous prediction of the friction level in the system. Friction levels of μ equal to 0.1 to 0.5 with an increment of 0.1 were simulated. The results indicated that a wrong prediction did make a difference. The maximum errors in order of increasing μ were 0.01692, 0.01862, 0.01, 0.01368, and 0.01845. A smaller system friction than predicted tends to cause overshoot while a larger system friction causes the response to be a little short. In the sinusoidal input response, the corrective torque was trying to correct the overshoot but its effectiveness was quite limited. This problem can be corrected by adaptive control action. Very often, the model-reference action was used with adaptive control.

H. EFFECT OF UNBALANCED SYSTEM

The effect of the out-of-balance appeared to be quite minimal as shown in Figures 4.30 through 4.32. The response typically reached a maximum values early on, usually within the first 0.12 seconds, then it dropped slowly as the acceleration reached maximum acceleration. After the platform reached the maximum acceleration and started to decelerate, the response rose again. As the distance between the center of gravity and the out of balance mass increased, the accuracy decreased. Therefore, It is important to consider the effect of out-of-balance mass in platform design.

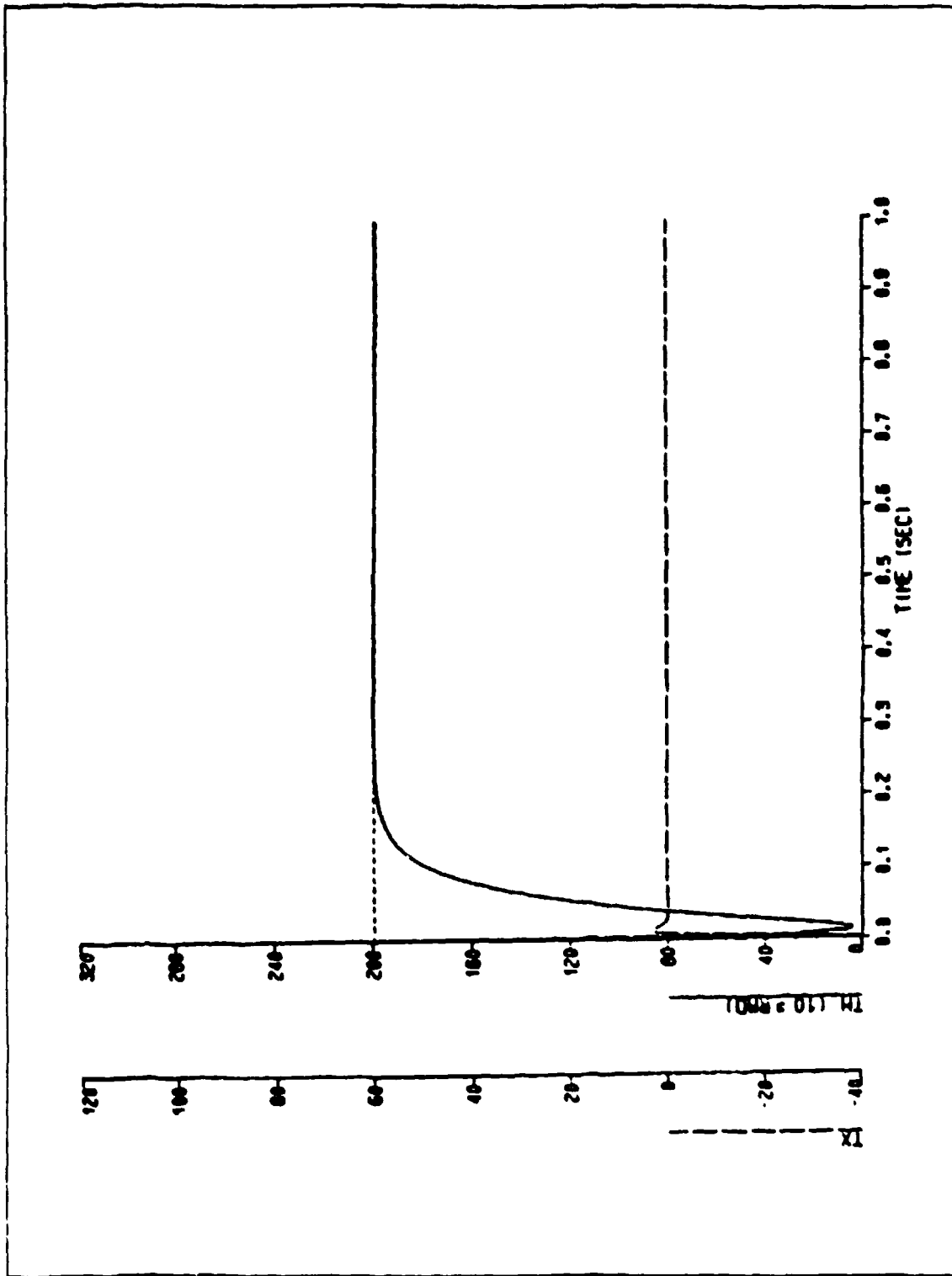


Figure 4.25 $\mu = 0.3$, $K_1 = 15.0$, $\delta = 0.05$, $\mu_m = 0.3$, $\delta_m = 0.05$, $G_1 = 3000.0$

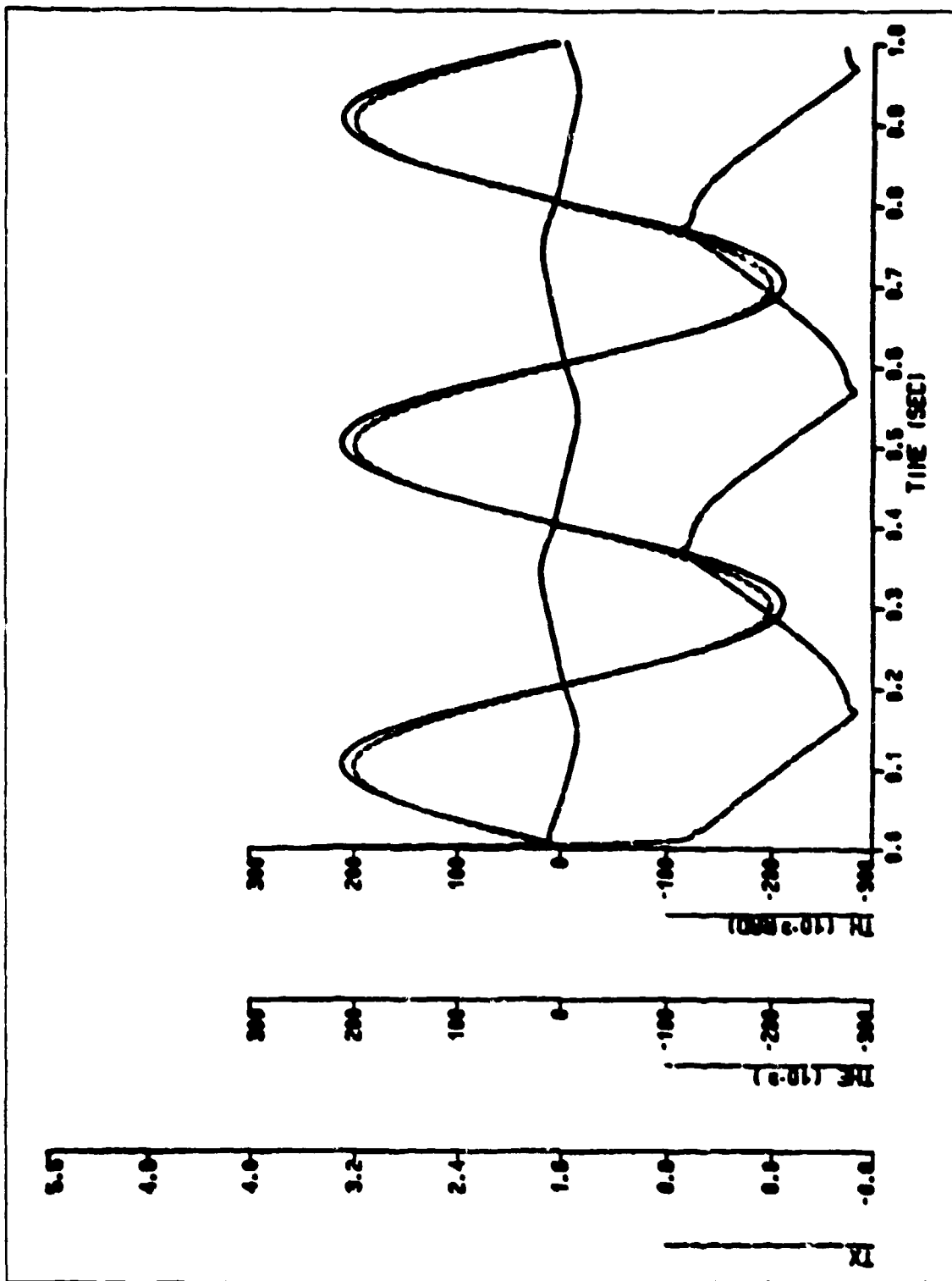


Figure 4.26 $\mu = 0.1$, $K_1 = 15.0$, $\delta = 0.05$, $\mu_m = 0.3$, $\delta_m = 0.05$, $G_1 = 3000.0$

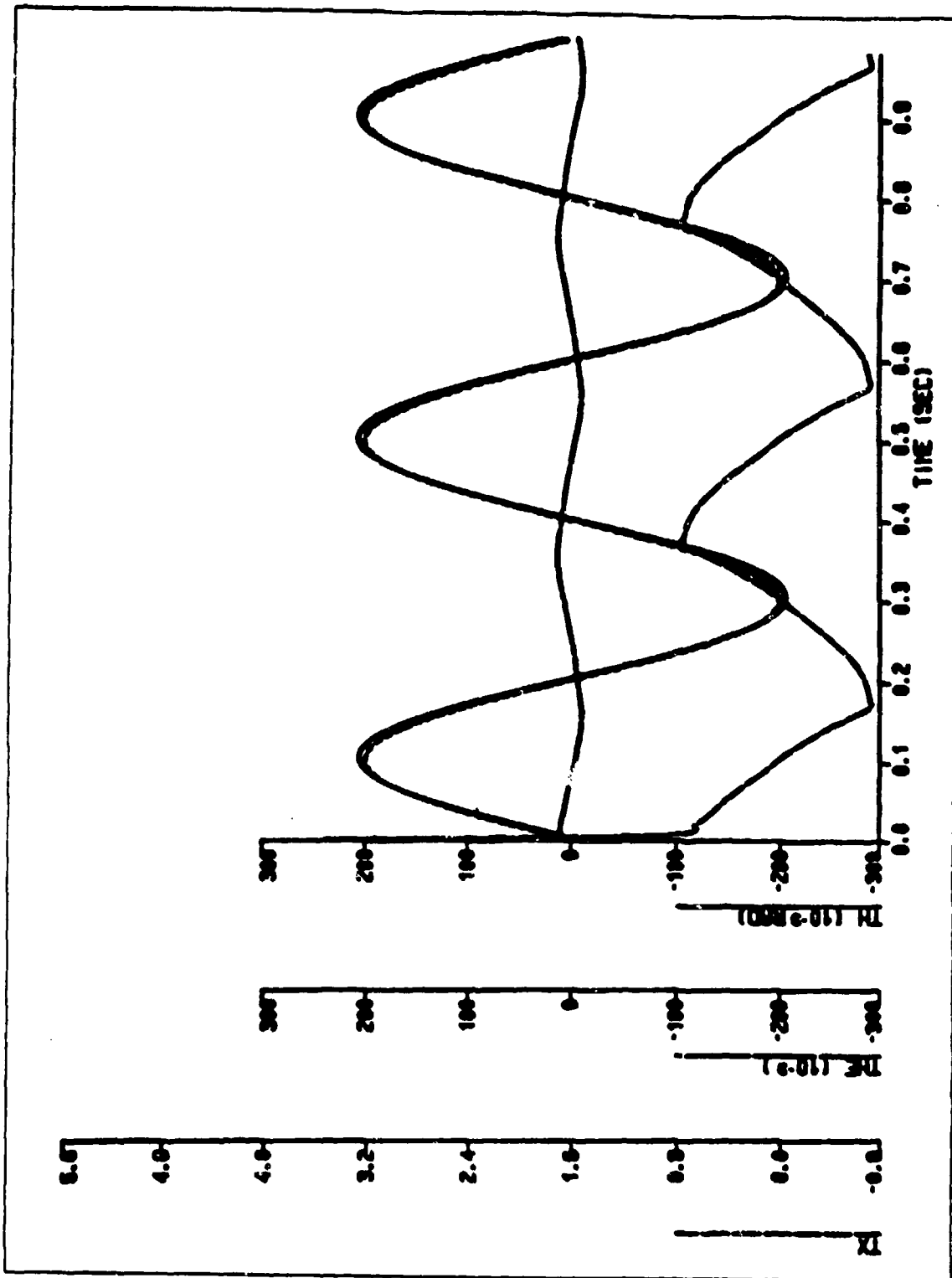


Figure 4.27 $\mu = 0.2$, $K_1 = 15.0$, $\delta = 0.05$, $\mu_m = 0.3$, $\delta_m = 0.05$, $G_1 = 3000.0$

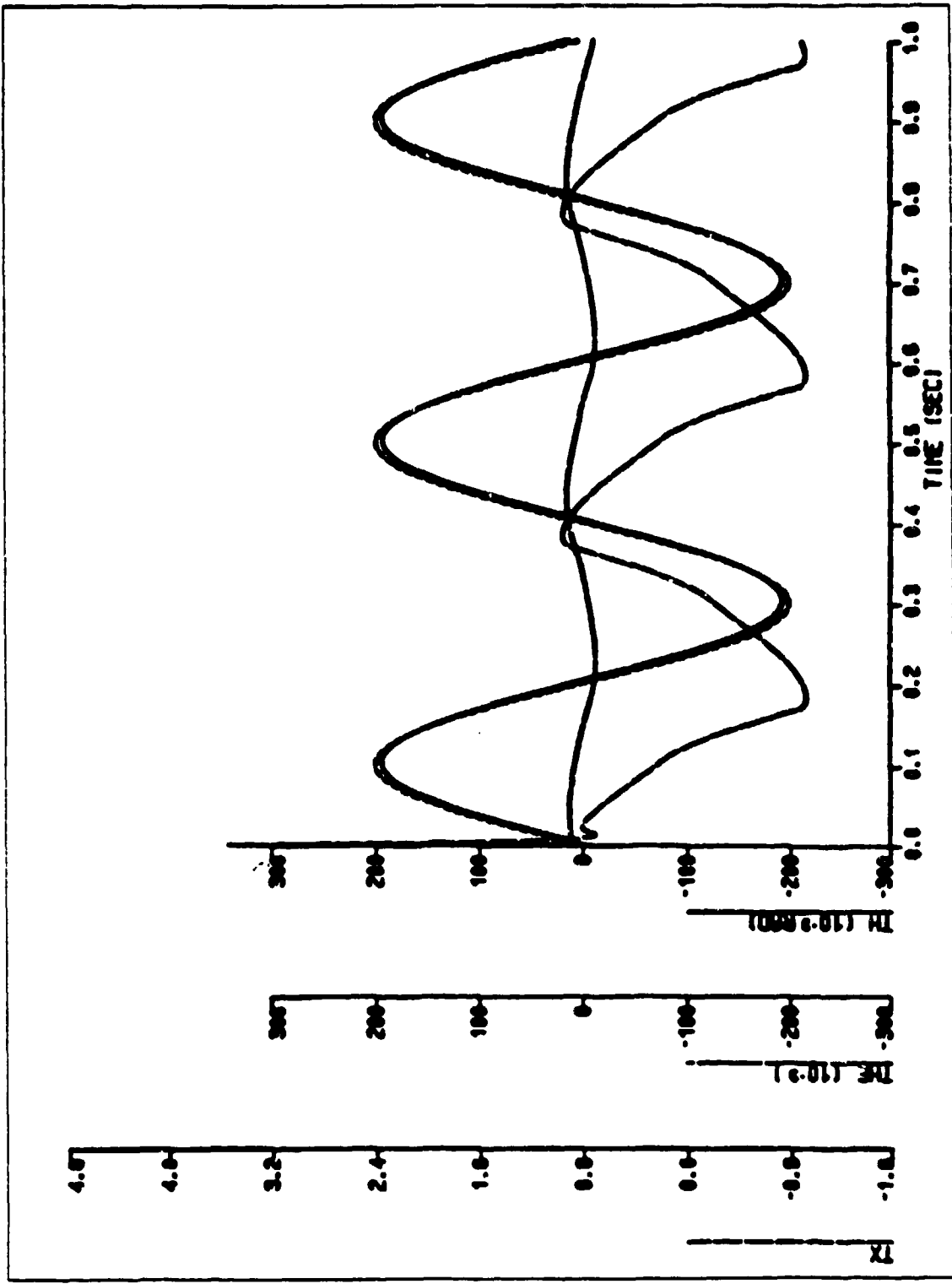


Figure 4.28 $\mu = 0.4$, $K_1 = 15.0$, $\delta = 0.05$, $\mu_m = 0.3$, $\hat{\sigma}_m = 0.05$, $G_1 = 3000.0$

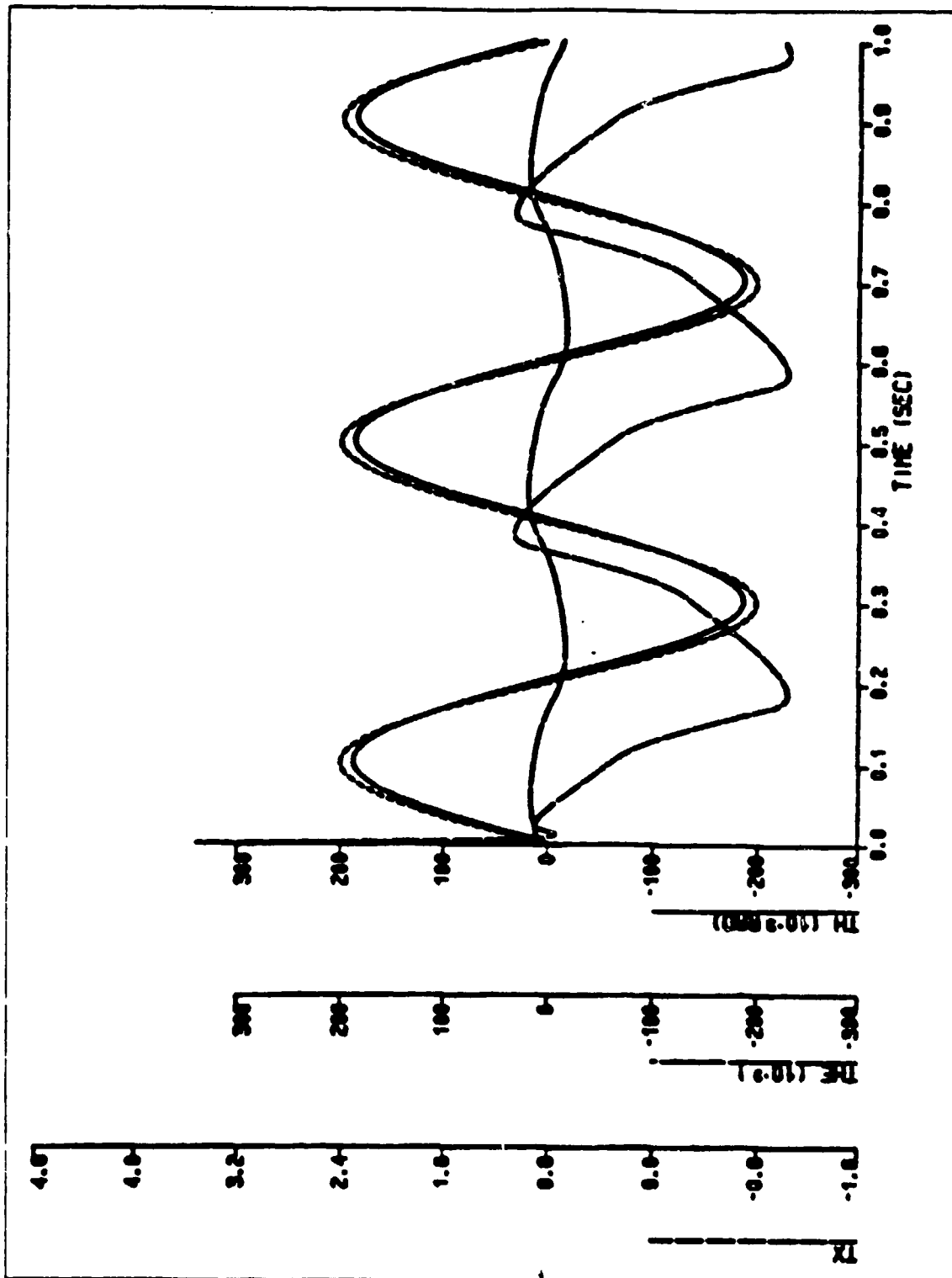


Figure 4.29 $\mu = 0.5$, $K_1 = 15.0$, $\delta = 0.05$, $\mu_m = 0.3$, $\delta_m = 0.05$, $G_1 = 3000.0$

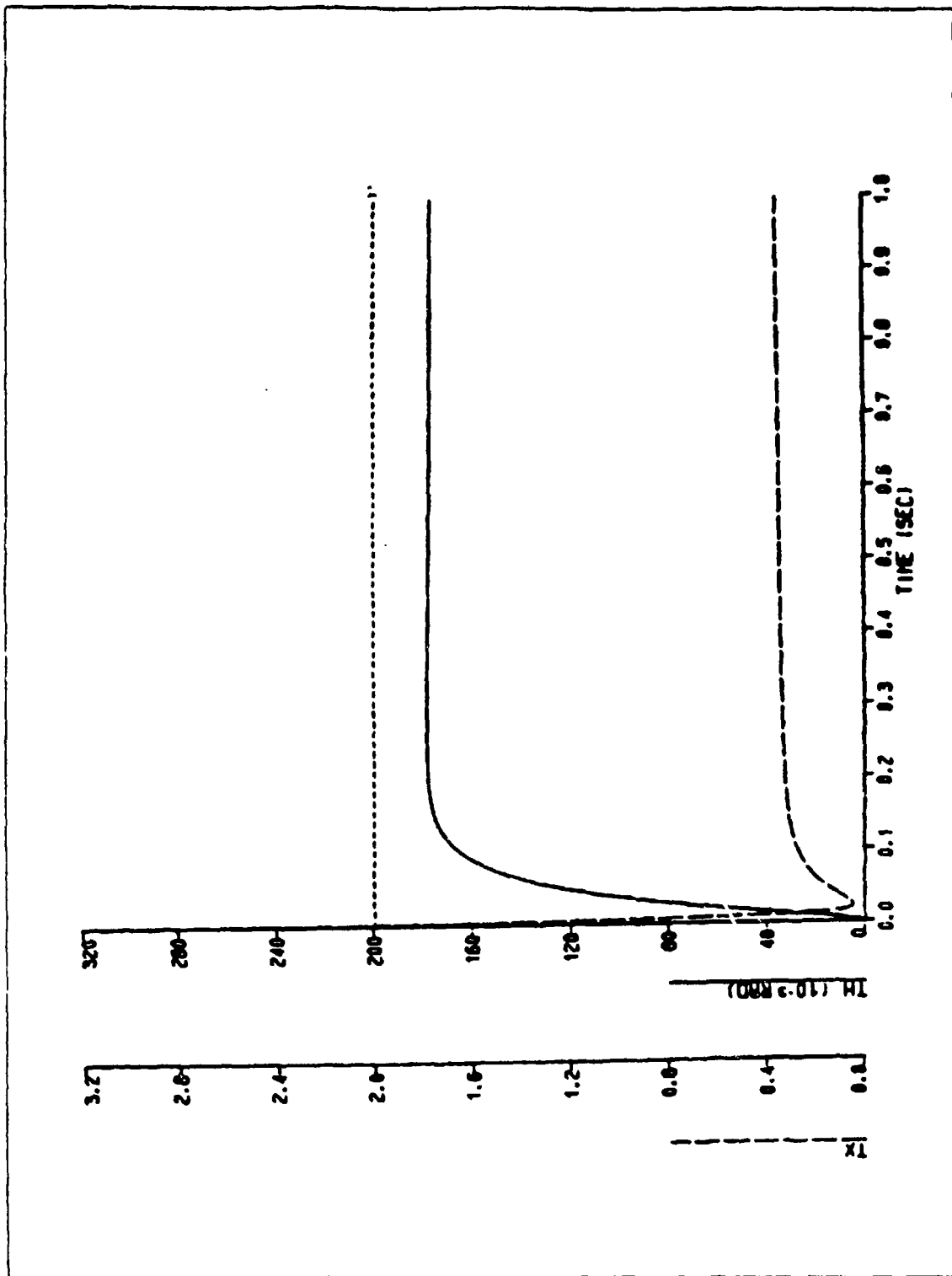


Figure 4.30 $\mu = 0.3$, $K_1 = 15.0$, $\delta = 0.05$, PD Control. $Z_m = 3864.0$, $Y_o = 0.1$, $Z_o = 0.2$

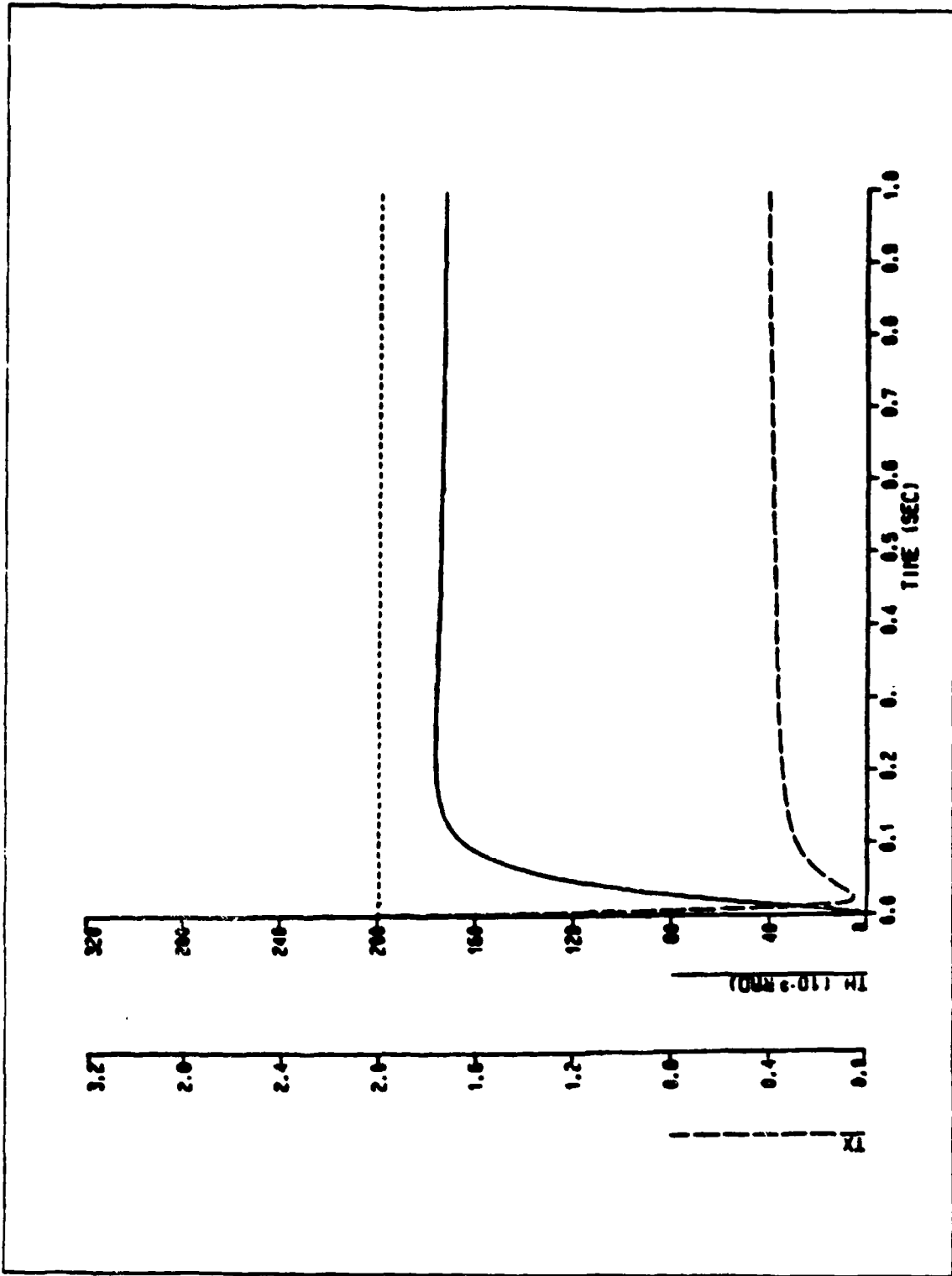


Figure 4.31 $\mu = 0.3$, $K_1 = 15.0$, $\delta = 0.05$, PD Control, $Z_m = 3864.0$, $y_o = 0.2$, $Z_o = 0.4$

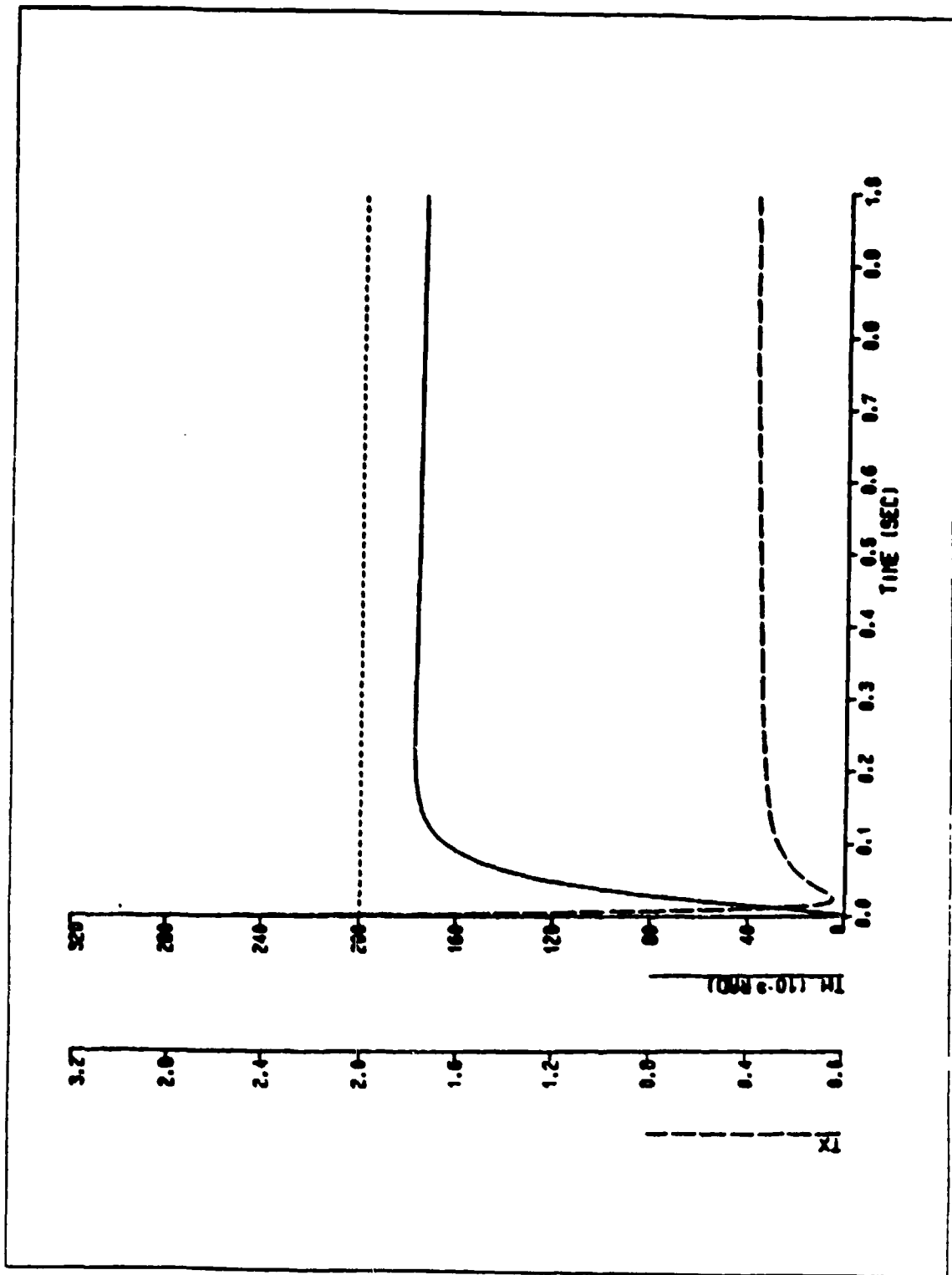


Figure 4.32 $\mu = 0.3$, $K_1 = 15.0$, $\delta = 0.05$, PD Control, $Z_m = 3864.0$, $y_o = 0.2$, $Z_o = 0.6$

I. EFFECT OF ACCELERATION

The effect of acceleration was similar to that of the C.G. location. The response began to drop as the acceleration approached maximum and recovered when the platform started to decelerate. This phenomenon was true for both the P.D. and model-reference control schemes shown in Figures 4.33 through 4.36 with either step input or sinusoidal input. However, the model-reference action allowed a much quicker recovery than the P.D. action. This was due to the correction torque provided by the model. Furthermore, the P.D. action had a much greater positional error while responded to a step input and a slower response to a sinusoidal input.

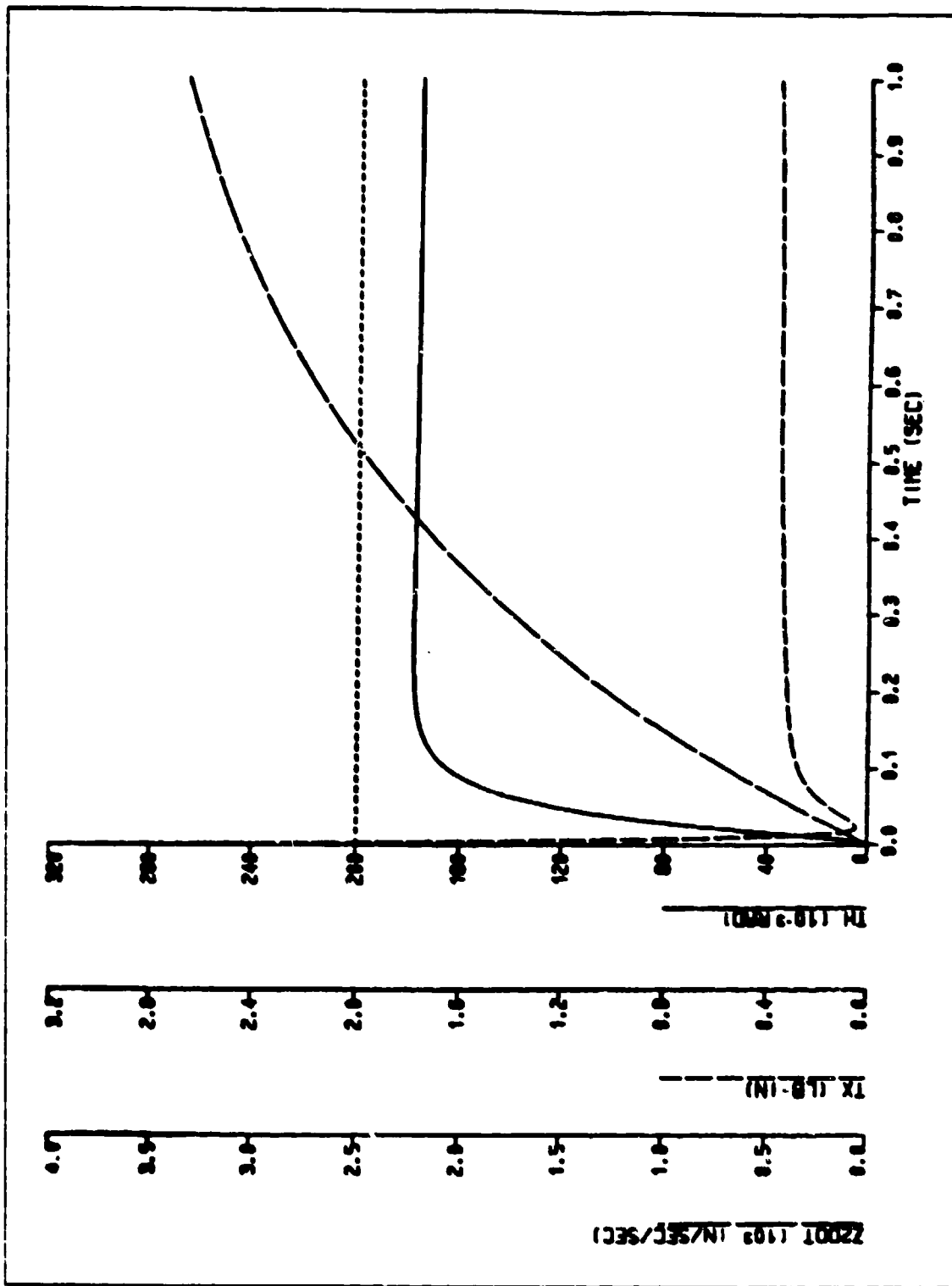


Figure 4.33 $\mu = 0.3$, $K_1 = 15.0$, $\delta = 0.05$, $Z_m = 3864.0$, PD Control, step response

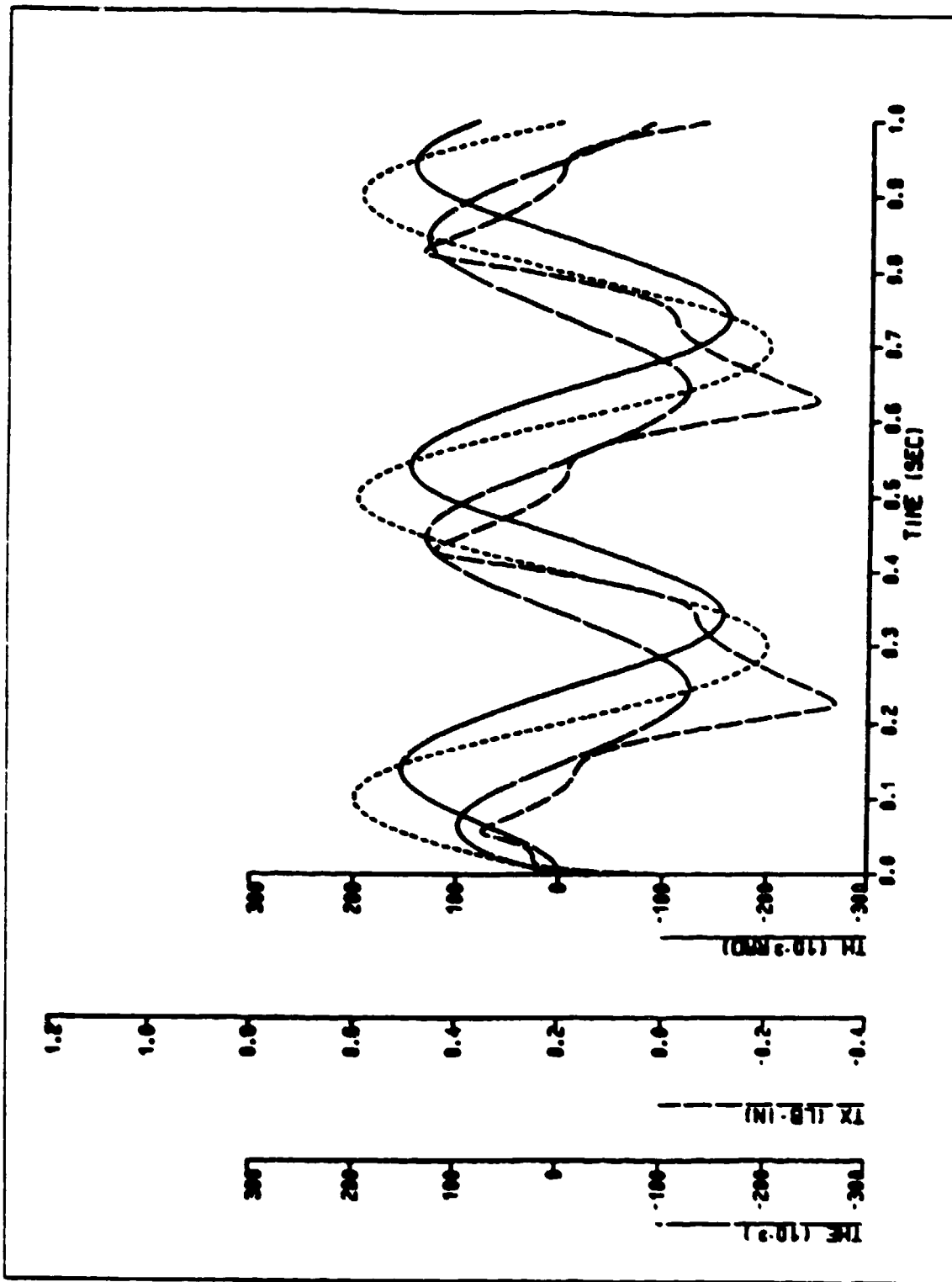


Figure 4.34 $\mu = 0.3$, $K_1 = 15.0$, $\delta = 0.05$, $Z_m = 3364.0$, PD Control, sin response

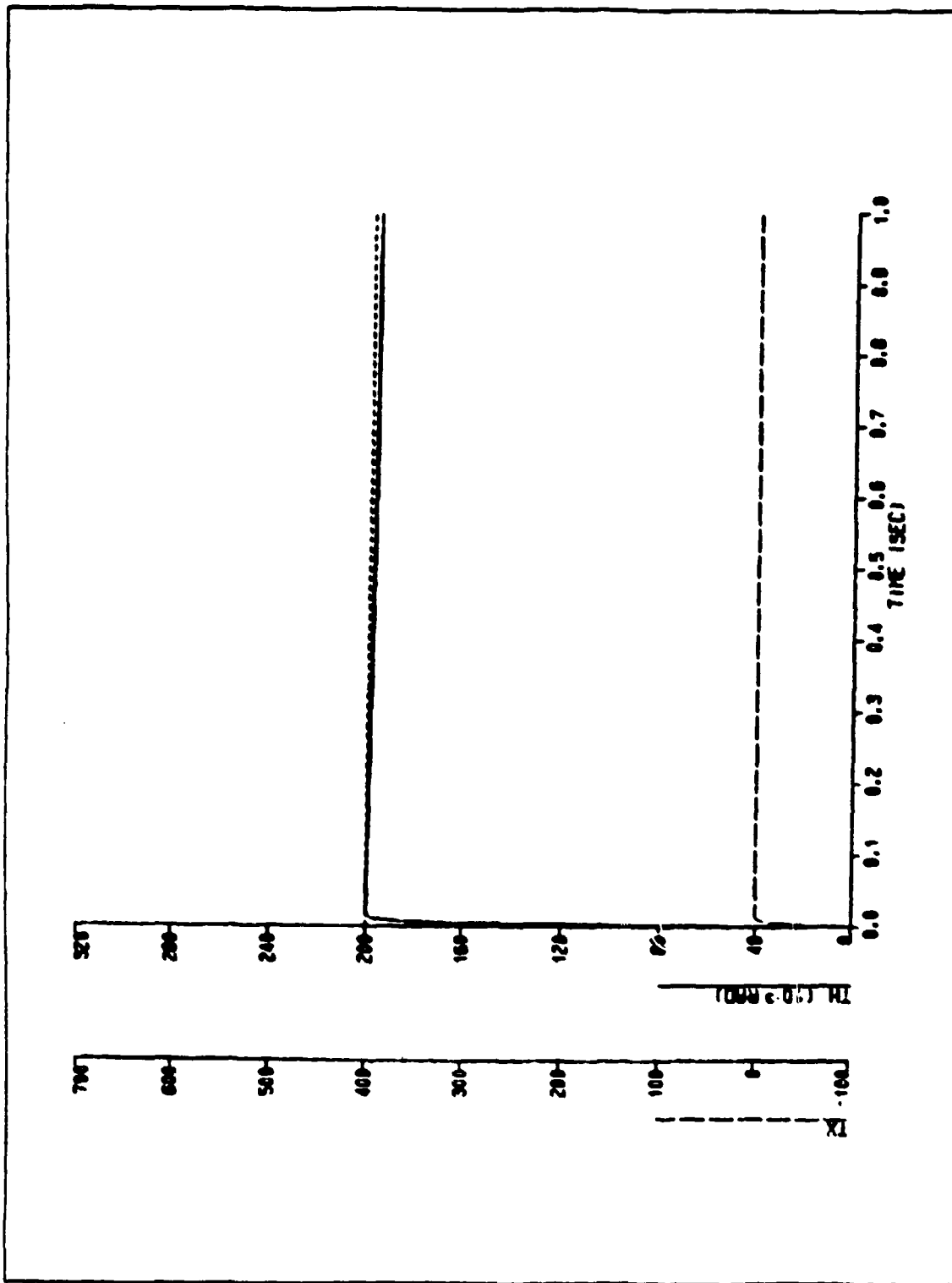


Figure 4.35 $\mu = 0.3$, $K_1 = 15.0$, $\delta = 0.05$, $Z_m = 3864.0$. M-F Control, step response

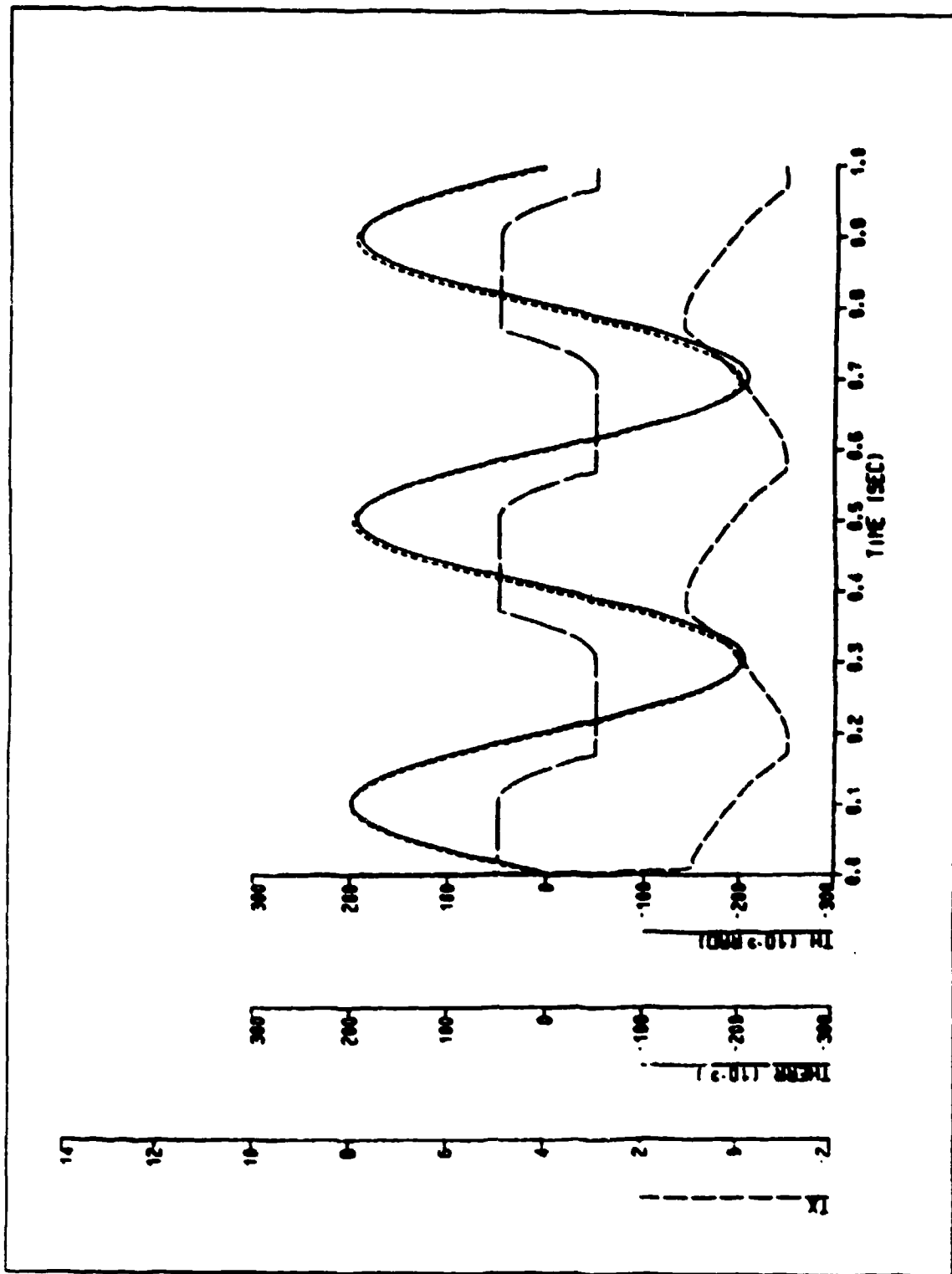


Figure 4.36 $\mu = 0.3$, $K_1 = 15.0$, $\delta = 0.05$, $Z_m = 3864.0$, M-F Control, sin response

V. DISCUSSION AND RECOMMENDATION

A. INTRODUCTION

This chapter summarizes the results obtained from the D.S.L. simulation and make recommendations for future work in this area.

B. DISCUSSION

The model-reference control method described here offered better tracking accuracy than either the P.D. or P.I.D. actions. It also minimized the problem of noisy feedback signals. This software based model utilizes an idealized model as a reference to predict the torque needed to overcome friction and gimbal dynamics and produce zero position error. First, the amount of torque needed to drive an idealized platform with no friction is predicted. Then, the torque required to overcome friction is determined from the friction model described in Chapter II. The sum of these two produced a predicted torque T_{xpred} . In addition, the idealized platform velocity \dot{X} is compared with the actual velocity $\dot{\theta}$ and the error is amplified. Similarly, the ideal position X is compared with the actual position θ and the error is amplified also. A corrective action occurs when these amplified error signals are added to T_{xpred} to yield the total required torque T_x . The result is a highly tuned, high accuracy, control action. Since the reference model is ideal, it does not have the draw back of large noise amplification as the other two control schemes do. Therefore, it is reasonable to expect better target tracking, even if the noise level is high.

The simulation results clearly shown the superior tracking accuracy provided by the model-reference method. The level of accuracy achieved is adequate for most target tracking seekers. Although this study was limited to the Y-Z plane only, this exercise did provide a better and clearer understanding of how friction and control variables affect the performance of the seeker. Of course, the performance of a missile seeker is affected by many other variables, not discussed here. The effect of vibration as the missile moves through the air, or the effect of air blast in the vicinity of the missile are examples of disturbance which will play an important role in the tracking accuracy of the missile. The friction model presented here is more realistic than simple coulomb friction model which produces an underfined friction force when $\dot{\theta}_j$ is equal to zero. The model presented here does allow non-zero friction force under stationary

conditions. Improvements can be made on the model-reference method to have adaptive capability to take into consideration the external disturbances, and variabilities in actual friction.

C. RECOMMENDATION

It is recommended that an experimental follow up be made to compare with the results obtained by analytical means. Frictional effect is not the only element affect seeker performance. There are other problem areas which also deserve the attention given here; among them vibration, shock, and random noise effects. It will be interesting to subject the model-reference control method described here to these external disturbances to see how well or how poor the current method handles these problem. These disturbances can be incorporated into the model-reference algorithm so their effects will be minimal. There are also an abundance of research in adaptive control. This type of control action enables a control system such as the one described here the ability to "learn and adjust" the model to different signal input. This latest technique is most versatile and would definitely contribute to the tracking accuracy of the seeker.

APPENDIX A
DSL LISTINGS (PD, PID CONTROL)

TITLE GIMBAL DYNAMICS

```

*****
*
*   AUTHOR:   JOSEPH CHAN
*   ABSTRACT: THIS PROGRAM SIMULATES THE MOTION OF A SINGLE
*   GIMBAL SYSTEM WHILE SUBJECTS TO STEP AND SINUSOIDAL
*   EXCITATIONS. PD AND PID CONTROL ACTION.
*

```

SYMBOLS:

```

*
*   BM       : MASS OF THE CYLINDER.
*   DELTA    : CHAR. DISP FOR COULOMB FRICTION MODEL.
*   F        : BEARING FRICTION FORCE.
*   IM       : MASS MOMENT OF INERTIA OF CYLINDER.
*   K1       : TORQUE GAIN CONSTANT.
*   K2       : VELOCITY FEEDBACK CONSTANT.
*   MU       : COEFFICIENT OF FRICTION.
*   PERIOD   : PERIOD OF THE SINE INPUT.
*   PH       : ANGLE BETWEEN THE Y-AXIS AND R.
*   R        : DISTANCE TO THE OFF-CENTER MASS FROM THE ORIGIN.
*   SM       : OUT OF BALANCE MASS.
*   TAU1     : ACCELERATION TIME CONSTANT (INITIAL PHASE).
*   TAU2     : ACCELERATION TIME CONSTANT (FINAL PHASE).
*   TH       : ANGULAR DISPLACEMENT OF THE CYLINDER.
*   TH0      : INITIAL ANGLE ROTATION.
*   TH2DOT   : ANGULAR ACCELERATION.
*   THCOM    : COMMAND ANGLE INPUT.
*   THD0     : INITIAL ANGULAR VELOCITY.
*   THDOT    : ANGULAR VELOCITY.
*   THE      : ANGULAR DISPLACEMENT OF THE CYLINDER.
*   THS      : POSITION OF THE SLIDER. (FRICTION MODEL)
*   TIME     : SIMULATION TIME.
*   TX       : MOTOR TORQUE.
*   Y0       : DISTANCE TO OFF CENTER-MASS IN THE Y DIRECTION.
*   Z0       : DISTANCE TO OFF CENTER-MASS IN THE Z DIRECTION.
*   Z2DOT    : LINEAR ACCELERATION.
*   ZM       : MAXIMUM LINEAR ACCELERATION.
*

```

GIMBAL PARAMETERS

```

*
*   CONST BM=0.00290, SM=0.00030, ZM=0.0000, IM=0.00370
*   LB-S**2/IN LB-S**2/IN IN/S**2 LB-IN-S**2
*
*   PARAM K1=15.000, MU=0.3, DELTA=0.05, PERIOD=0.4
*   LB-IN/RAD IN IN SEC SEC RAD
*
*   PARAM Y0=0.1, Z0=0.2, TAU1=0.5, TAU2=0.5, THMAX=0.2
*   IN IN IN IN IN
*

```

```

*
*   INITIAL
*   R      = SQRT(Y0**2+Z0**2)
*   PH     = ACOS(Y0/R)
*   K2     = SQRT(8*IM*K1)
*   F      = 0.0
*   TH     = 0.0
*   TH0    = 0.0

```

```

THD0 = 0.0
THDOT = 0.0
THE = 0.0
THEO = 0.0
THERR = 0.0
THS = 0.0

```

*

DYNAMIC

*

```

*****
*                                     ACCELERATION PROFILE *
*****

```

```

T1 = TIME-4.0*TAU1
Z2DOT := ZM*(1.0-EXP(-TIME/TAU1))
IF (TIME.GT.(4.0*TAU1)) THEN
  Z2DOT = ZM*EXP(-T1/TAU2)
ENDIF

```

*

* SINUSOIDAL EXCITATION

*

```
# THCOM=THMAX*SIN(2*PI*TIME/PERIOD)
```

*

* STEP INPUT

*

```
THCOM=THMAX
```

*

DERIVATIVE

NOSORT

*

```

*****
*                                     BEARING FRICTION MODEL *
*****

```

```

THERR = TH-THS
F = MU*(THERR)/DELTA
IF ((ABS(F)).LT.MU) THS = THS
IF ((ABS(F)).GT.MU) THS = TH-DELTA*F/ABS(F)

```

*

```

*****
*                                     MOTOR TORQUE MODEL *
*****

```

```
THE = THCOM-TH
```

*

* PD FEEDBACK

*

```
# TX = K1*(THE)-K2*(THDOT)
```

*

* PID FEEDBACK

*

```

TX = K1*(THE)-K2*THDOT+(K1/TI)*Y
TH2DOT = (TX-F-SM*Z2DOT*R*(COS(TH)*COS(PH)-SIN(TH) ...
          *SIN(PH)))/(IM+SM*R**2)
THDOT = INTGRL(THD0,TH2DOT)
TH = INTGRL(TH0,THDOT)
# Y = INTGRL(TH0,THE)

```

*

```
METHOD RK5
CONTRL FINTIM=1.00, DELT=0.001
```

*

```

*****
*                                     PRINT RESULTS *
*****

```

```
SAVE 0.001, TX, F, THCOM, TH, THE, THERR
PRINT 0.010, TX, F, THCOM, TH, THE, THERR
```

*

* THETA VS TIME

*

```
#GRAPH (A,DE=TEK618) TIME(LE=8,UNIT='SEC') TH(LO=-.3,SC=.1,NI=6, ...
```

```

#      UN='RAD') THCOM(AX=OMIT,LO=-.3,SC=0.1,NI=6,LI=4,UN='RAD') ...
#      THE(LO=-.3,SC=.1,NI=6,LI=2), TX(LI=3,UN='LB-IN')
GRAPH (A,DE=TEK618) TIME(LE=8,UNIT='SEC') TH(LO=0.0,SC=.04,NI=8, ...
      UN='RAD') THCOM(AX=OMIT,LO=0.0,SC=0.04,NI=8,LI=4,UN='RAD') ...
      TX(LI=3,UN='LB-IN')
LABEL (A) MU=0.3, K1=15.0, DELTA=0.05
*
* THETA VS TIME WITH THETA COMMAND AS REFERENCE (SINE INPUT)
*
#GRAPH (A,DE=TEK618) TIME(LE=8,UNIT='SEC') TH(LO=-0.3,SC=0.1,NI=6, ...
#      UN='RAD') THCOM(LO=-0.3,SC=0.1,NI=6,LI=4,UN='RAD')
*
* HYSTERISIS
*
#GRAPH (B,DE=TEK618) TH(LE=8,PO=2,4,AX=LIN,DRAW,UN=RAD) F(UN='LB')
#LABEL (A,B) MU=0.25, K1=2.00, K2=0.05, DELTA=0.050
*
* TIME RESPONSE
*
#GRAPH (C,DE=TEK618) TIME(LE=8,UN='SEC') TH(LO=-.3,SC=.1,NI=6, ...
#      LI=1,UN='RAD') THS(LO=-.3,SC=.1,NI=6,LI=2,UN='RAD') ...
#      F(LO=-.3,SC=.1,NI=6,LI=4,UN='LB')
#LABEL (C) TIME HISTORY
*
END
STOP

```

APPENDIX B
DSL LISTINGS (PC CONTROL)

TITLE GIMBAL DYNAMICS2

```

*****
*
*   AUTHOR:   JOSEPH CHAN
*   ABSTRACT: THIS PROGRAM SIMULATES THE MOTION OF A SINGLE
*   GIMBAL SYSTEM SUBJECTS TO STEP AND SINUSOIDAL EXCITATIONS
*   USING PREDICTION CORRECTION CONTROL ACTION.
*
*-----*

```

```

*
*   SYMBOLS:
*
*   BM      : MASS OF THE CYLINDER.
*   DELTA   : CHAR. DISP FOR COULOMB FRICTION MODEL.
*   DELTAM  : CHAR. DISP FOR COULOMB FRICTION (REFERENCE MODEL).
*   F       : BEARING FRICTION FORCE.
*   FM      : BEARING FRICTION FORCE (REFERENCE MODEL).
*   G1      : REFERENCE MODEL TRANSFER FUNCTION.
*   G2      : REFERENCE MODEL TRANSFER FUNCTION.
*   IM      : MASS MOMENT OF INERTIA OF CYLINDER.
*   K1      : TORQUE GAIN CONSTANT.
*   K2      : VELOCITY FEEDBACK CONSTANT.
*   MU      : COEFFICIENT OF FRICTION.
*   MUM     : COEFFICIENT OF FRICTION (REFERENCE MODEL).
*   PH      : ANGLE BETWEEN THE Y-AXIS AND R.
*   R       : DISTANCE TO THE OFF-CENTER MASS FROM THE ORIGIN.
*   SM      : OUT OF BALANCE MASS.
*   TAU1    : ACCELERATION TIME CONSTANT (INITIAL PHASE).
*   TAU2    : ACCELERATION TIME CONSTANT (FINAL PHASE).
*   TH      : ANGULAR DISPLACEMENT OF THE CYLINDER.
*   TH0     : INITIAL ANGLE ROTATION.
*   TH2DOT  : ANGULAR ACCELERATION.
*   THCOM   : CONTROL ANGLE INPUT.
*   THDO    : INITIAL ANGULAR VELOCITY.
*   THDOT   : ANGULAR VELOCITY.
*   THE     : ANGULAR DISPLACEMENT OF THE CYLINDER.
*   THS     : POSITION OF THE SLIDER. (FRICTION MODEL)
*   TIME    : SIMULATION TIME.
*   TX      : MOTOR TORQUE.
*   TXPRED  : MOTOR TORQUE (PREDICTED)
*   X       : DISTANCE OF MASS AT ANY TIME T. (FRICTION MODEL)
*   X0      : INITIAL DISTANCE OF REFERENCE MODEL.
*   X1      : DISTANCE MOVED BY THE SLIDER. (FRICTION MODEL)
*   X2DOT   : ACCELERATION OF REFERENCE MODEL.
*   XDOT    : VELOCITY OF REFERENCE MODEL.
*   XDOT0   : INITIAL VELOCITY OF REFERENCE MODEL.
*   XS      : POSITION OF SLIDER (REFERENCE MODEL).
*   YO      : DISTANCE TO OFF CENTER-MASS IN THE Y DIRECTION.
*   ZO      : DISTANCE TO OFF CENTER-MASS IN THE Z DIRECTION.
*   Z2DOT   : LINEAR ACCELERATION.
*   ZM      : MAXIMUM LINEAR ACCELERATION.

```

```

*****
*
*   GIMBAL PARAMETERS
*
*-----*
*
*   CONST BM=0.00290, SM=0.00030, ZM=0.0000, IM=0.00370
*   LB-S**2/IN   LB-S**2/IN   IN/S**2   LB-IN-S**2
*
*   PARAM K1=150000, MU=0.3, DELTA=0.05, PERIOD=0.4

```

```

*      LB-IN/RAD              IN              SEC/CYC
*
PARAM G1=500.00,  MUM=0.3,  DELTAM=0.05,  THMAX=0.2
*                      IN                      RAD
*
PARAM YO=0.1,  ZO=0.2,  TAU1=0.5,  TAU2=0.5
*      IN      IN      SEC      SEC
*
INITIAL
R      = SORT(YO**2+ZO**2)
PH     = ACOS(YO/R)
K2     = SORT(8*IM*K1)
G2     = SORT(8*IM*G1)
F      = 0.0
TH     = 0.0
THO    = 0.0
THDO   = 0.0
THDOT  = 0.0
THE    = 0.0
THEO   = 0.0
THERR  = 0.0
THS    = 0.0
X      = 0.0
XO     = 0.0
XDOT   = 0.0
XDOTO  = 0.0
X2DOT  = 0.0
XS     = 0.0
*
DYNAMIC
*
*****
*      ACCELERATION PROFILE      *
*****
*
T1     = TIME-4.0*TAU1
Z2DOT  = ZM*(1.0-EXP(-TIME/TAU1))
IF (TIME.GT.(4.0*TAU1)) THEN
Z2DOT  = ZM*EXP(-T1/TAU2)
ENDIF
*
* SINUSOIDAL EXCITATION
*
#      THCOM=THMAX*SIN(2*PI*TIME/PERIOD)
*
* STEP INPUT
*
      THCOM=THMAX
*
DERIVATIVE
NOSORT
*
*****
*      MODEL REFERENCE DYNAMICS      *
*****
*
U      = (THCOM-X)*G1-G2*XDOT
X2DOT  = U/(IM+SM*R**2)
FM     = MUM/DELTAM*(X-XS)
IF ((ABS(FM)).LT.MUM) XS = XS
IF ((ABS(FM)).GT.MUM) XS = X-DELTAM*FM/ABS(FM)
TXPRED = U+FM
*
*****
*      BEARING FRICTION MODEL      *
*****
*
THERR  = TH-THS
F      = MU*(THERR)/DELTAM
IF ((ABS(F)).LT.MU) THS = THS

```

```

IF ((ABS(F)).GT.MU) THS = TH-DELTA*F/ABS(F)
*
*****
*
*           MOTOR TORQUE MODEL
*           (PREDICTOR CORRECTOR METHOD)
*
*****
THE      = THCOM-TH
TX       = TXPRED+K1*(X-TH)+K2*(XDOT-THDOT)
IF (TX.GT.55.0) TX=55.0
TH2DOT  = (TX-F-SM*Z2DOT*R*(COS(TH)*COS(PH)-SIN(TH) ...
           *SIN(PH)))/(IM+SM*R**2)
THDOT   = INTGRL(THD0,TH2DOT)
TH      = INTGRL(TH0,THDOT)
X       = INTGRL(X0,XDOT)
XDOT    = INTGRL(XDOT0,X2DOT)
METHOD  RK5
CONTRL  FINTIM=1.00, DELT=0.0001
*
*****
*
*           PRINT RESULTS
*
*****
SAVE 0.001, TX, TXPRED, F, THCOM, TH, THE, THERR
PRINT 0.010, TX, TXPRED, F, THCOM, TH, THE, THERR
*
* THETA VS TIME
*
#GRAPH (A,DE=TEK618) TIME(LE=8,UNIT='SEC') TH(LO=-.3,SC=.1,NI=6, ...
# UN='RAD') THCOM(AX=OMIT,LO=-.3,SC=0.1,NI=6,LI=4,UN='RAD') ...
# THERR(LO=-.3,SC=.1,NI=6,LI=2), TX(LI=3)
GRAPH (A,DE=TEK618) TIME(LE=8,UNIT='SEC') TH(LO=0.0,SC=.04,NI=8, ...
UN='RAD') THCOM(AX=OMIT,LO=0.0,SC=0.04,NI=8,LI=4,UN='RAD') ...
TX(LI=3)
LABEL (A) MU=0.3, K1=1000, DELTA=0.05, MUM=0.3, DELTAM=0.05, G1=1000
*
* THETA VS TIME WITH THETA COMMAND AS REFERENCE (SINE INPUT)
*
#GRAPH (A,DE=TEK618) TIME(LE=8,UNIT='SEC') TH(LO=-0.3,SC=0.1,NI=6, ...
# UN='RAD') THCOM(LO=-0.3,SC=0.1,NI=6,LI=4,UN='RAD')
*
* HYSTERISIS
*
#GRAPH (B,DE=TEK618) TH(LE=8,PO=2,4,AX=LIN,DRAW,UN=RAD) F(UN='LB')
#LABEL (A,B) MU=0.25, K1=2.00, K2=0.05, DELTA=0.050
*
* TIME HISTORY
*
#GRAPH (C,DE=TEK618) TIME(LE=8,UN='SEC') TH(LO=-.3,SC=.1,NI=6, ...
# LI=1,UN='RAD') THS(LO=-.3,SC=.1,NI=6,LI=2,UN='RAD') ...
# F(LO=-.3,SC=.1,NI=6,LI=4,UN='LB')
#LABEL (C) TIME HISTORY
*
END
STOP

```

LIST OF REFERENCES

1. Walrath, C.D., "Adaptive Bearing Friction Compensation Based on Recent Knowledge of Dynamic Friction," *Automatica*, v. 10, n.6, pp. 717-727, 1984.
2. Landau, I.D., "A Survey of Model Reference Adaptive Techniques-Theory and Applications" *Automatica*, v. 10, pp. 353-379, 1974.
3. Slotine, J.J.E. "The Robust Control of Robot Manipulators" *International Journal of Robotic Research*, v. 4, n. 2, 1985.
4. **Dynamic Simulation Language/VS, Language Reference Manual, Program Number 5798-PXJ (SH20-6288-0), First Edition, IBM Corporation, June 1984.**
5. **Dynamic Simulation Language/VS, Program Description: Operation Manual, Program Number 5798-PXJ (SH20-6287-0), First Edition, IBM Corporation, June 1984.**

INITIAL DISTRIBUTION LIST

	No. Copies
1. Defense Technical Information Center Cameron Station Alexandria, VA 22304-6145	2
2. Library, Code 0142 Naval Postgraduate School Monterey, CA 93943-5002	2
3. Naval Weapons Center Head, Code 394 China Lake, CA 93555-6001	1
4. Naval Weapons Center Head, Code 3941 China Lake, CA 93555-6001	1
5. Chairman, Mechanical Engineering Naval Postgraduate School Code 69 Monterey, CA 93943-5002	4
6. Prof. L. W. Chang, Prof. Code 69CK Naval Postgraduate School Monterey, CA 93943-5002	1
7. Mr. Joseph Chan Naval Weapons Center Code 3941 China Lake, CA 93555-6001	5
8. Mr. R. Werneth N.S.W.C. Code U25 White Oak, MD 20910	1